ORIGINAL ARTICLE

lajss.org© Latin American Journal of Solids and Structures

www.lajss.org

Second–order models for the bending analysis of thin and moderately thick circular cylindrical shells

Clifford Ugochukwu Nwoji[a], **Deval Godwill Ani**[b*]

[a]Department of Civil Engineering, Alex Ekwueme Federal University, Ndufu-Alike, Ebonyi state, Nigeria. Email: ugo.nwoji@unn.edu.ng
[b]Department of Civil Engineering, University of Nigeria, Nsukka, Enugu state, Nigeria. Email: deval.ani.pg00727@unn.edu.ng, anidevalgodwill@gmail.com

* Corresponding author

https://doi.org/10.1590/1679-78256843

Abstract

The suitability of employing the second-order shear deformation theory to static bending problems of thin and moderately thick isotropic circular cylindrical shells was investigated. Two variant forms of the polynomial second-order displacement models were considered. Both models account for quadratic expansions of the surface displacements along the shell thickness, although the second model (SSODM) was augmented by the initial curvature term. The equilibrium equations were derived by use of the principle of virtual work. Navier analytical solutions were obtained under simply supported boundary conditions. The results of the displacements and stresses revealed that the theory formulated on the SSODM provides a good depiction of the bending response of thin and moderately thick shells and are in close agreement with those of the first and higher-order shear deformation theories (FSDT; HSDT). The ability of the theory formulated on the first model (FSODM) to predict adequate values of displacements and stresses in thin shells was found to be significantly affected by changes in length to radius of curvature (*l*/*a*) ratios.

Keywords

Isotropic material; thin and moderately thick shells; shear deformation theory; polynomial second-order displacement models; circular cylindrical shells; bending analysis; simply supported boundaries.

Graphical Abstract

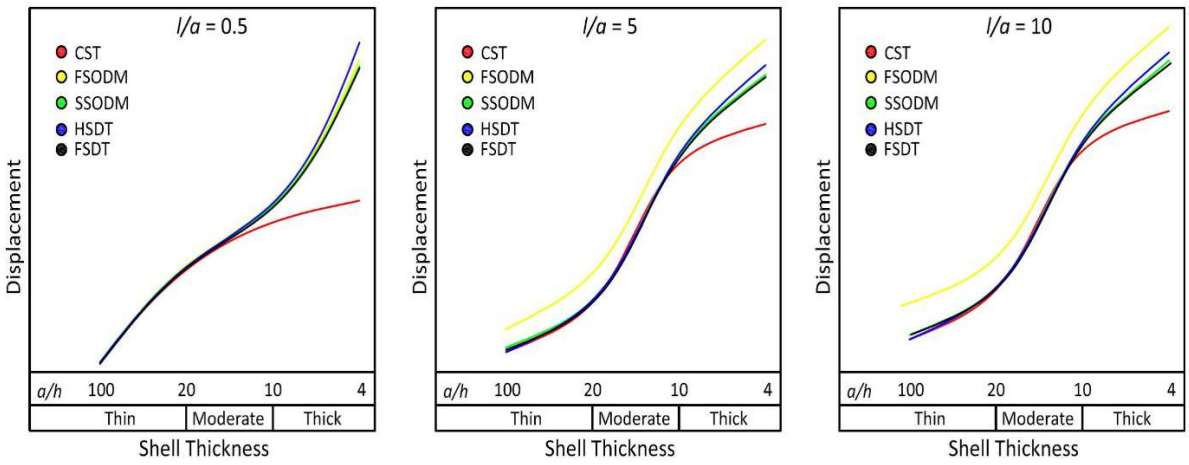

Received November 10, 2021. In revised form February 15, 2022. Accepted March 07, 2022. Available online March 11, 2022
https://doi.org/10.1590/1679-78256843

Latin American Journal of Solids and Structures. ISSN 1679-7825. Copyright © 2021. This is an Open Access article distributed under the terms of the Creative Commons Attribution License, which permits unrestricted use, distribution, and reproduction in any medium, provided the original work is properly cited.

1 INTRODUCTION

Shells are three dimensional (3D) material solids bounded by two closely spaced arbitrary curved surfaces. Structural shells are known for possessing great capacity in carrying external loading on account of their high strength and rigidity. The curved geometry of the shell permits the development of in-plane membrane forces which acts as the dominant resistance to imposed loading in thin shells, and together with its continuity, the shell can transfer this loading in different directions without the help of a moment frame. Thus, the shell possesses a broad mechanical advantage over other structural elements. Shells are categorized as singly curved, doubly curved and combined shells. The cylindrical shell has received the most attention among the singly curved shells and its everyday application includes being used as liquid transport and storage facilities. These shells are also utilized in covering large spaces such as roofs of buildings, garages and warehouses, in cases where no interior roof supporting elements (columns and walls) are needed. Most studies on the static bending (flexural) behavior of elastic isotropic shells are formulated on the kinematic hypothesis of Love – Kirchhoff, in which the transverse shear effect on the deformation of the elastic shell is neglected. An assumption proven to be reasonable when applied to thin isotropic shells with thickness to radius ratio $h/R_i \leq 1/20$ (Ugural, 2010). The classical (Love – Kirchhoff) shell theories have been found to provide excellent results with regards to the bending, dynamic and buckling responses of isotropic thin shells subject to external loading. Although, for shells considered thick, utilized mostly on account of obtaining increased flexural (torsional) rigidity, especially in cases where the shell span, loading or induced deflection are significantly large, likewise, in cases where the shell is of an anisotropic or composite material, the neglect of the transverse shear in modeling the response (static or dynamic) of these laminated composites or thick shells to external forces by the classical shell theories (CSTs) leads to considerable errors in deflections and fundamental frequencies. On this regard, first and higher-order shear deformation theories had been developed with the aim of improving upon the limitations in application associated with the Love – Kirchhoff hypothesis and extending the classical shell theory to thick isotropic and anisotropic structural shells.

The first-order shear deformation theories initiated by Mindlin (1951) using a displacement based approach accounts for transverse shear deformation by postulating that: the straight normals to the reference (middle) surface would still remain straight even after deformation occurs, but are now no longer required to lie normal to the deformed reference surface. These first-order shear deformation theories (FSDTs) had been found to be quite accurate in the estimation of parameters like deflection and fundamental frequencies. However, the first-order theories which expand the surface displacements as linear functions of the thickness coordinate result in a constant through thickness distribution of the transverse shear, which as a consequence fails to satisfy the zero transverse shear/traction requirements on the top and bottom boundary surfaces of the shell. The above phenomenon is found to be in contradiction to the parabolic distribution of the transverse shear as required by the theory of elasticity, hence necessitating the need for the introduction of transverse shear correction factors in order to correct this abnormality. These setbacks however, had been remedied by the higher-order shear deformation theories (HSDTs), which are based on displacement models generated from the Taylor series expansion of the surface displacements as higher order functions of the thickness coordinate truncated at the desired order. Albeit introducing additional mathematical complexities with increasing order of expansion. These higher-order expansions have been utilized in both linear and non-linear structural shell studies. Higher-order expansions employed in linear shell studies can be found in works by Reddy and Liu (1985), Soldatos (1986), Di and Rothert (1995) and Cho, Kim and Kim (1996). Non-linear higher-order shell theories, in which the non-linear terms in the kinematic parameters are retained, are presented in works by Amabili and Reddy (2010, 2020). The higher-order expansions truncated at the third-order has been the most utilized in modeling the transverse shear deformation in isotropic, laminated composites and functionally graded materials by many researchers. This is as a consequence of its ease of transformation to satisfy requirements like the need for a traction free upper and lower boundary surfaces of the beam, plate or shell element without necessarily having to refer to the particular element's equilibrium equations associated with 3D elasticity, and also due to the fact that the parabolic distribution of the transverse shear can easily be achieved by these constrained third-order displacement models as found in Reddy (1984), Reddy and Liu (1985) and Onyeka et al. (2018). The constrained displacement model of third-order expansions of the surface displacements as proposed by Reddy and Liu (1985) had successfully been utilized by Oktem and Chaudhuri (2007) to study the deformation of shallow moderately thick cross-ply doubly curved panels of finite dimensions; Harle and Asha (2013) to investigate the buckling and vibratory response of laminated cross-ply circular cylindrical panels; and more recently by Nwoji et al. (2021) to study the effect of transverse shear deformation on the static flexural behavior of isotropic circular cylindrical shells through varying length to radius of curvature ratios (l/a). In the work by Oktem and Chaudhuri (2007), a previously unavailable Levy-type solution procedure was used to obtain the analytical solutions of the deformation problem. The constrained form of the third-order displacement model which satisfied the zero transverse shear surface condition was also used by Lim and Liew (1995) to study the dynamic

characteristics of isotropic cylindrical shallow shells and by Soldatos (1986) to study the free vibration problem of moderately thick isotropic oval cylindrical shells. In the studies conducted by Di and Rothert (1995) and Cho et al. (1996) on the deformation of laminated composite cylindrical shells, an unconstrained third-order displacement model superimposed by a zig – zag linear function was adopted in order to obtain a parabolic distribution of the transverse shear that satisfies the requirements of a stress free laminate surface as well as continuity of the transverse shear stresses on the interface between the laminate surfaces. Di and Rothert (1995) however attained these requirements by use of the equilibrium equations associated with three – dimensional (3D) elasticity. Ali, Alsubari and Aminanda (2015) also considered an unconstrained third-order displacement model augmented by a zig – zag function to investigate the effect of moisture and temperature on the bending deformation of cross-ply laminated simply supported cylindrical shell strips. The HSDTs have generally been found to result in more acceptable through thickness distribution of the transverse shear strains; together with satisfying the traction free surface condition, hence these theories avoid the utilization of shear correction coefficients and have been known to provide excellent numerical results when employed in the analysis of thin and moderately thick beams, plates and shells.

The series expansion truncated at the second-order has been used by many researchers to extend the classical Love – Kirchhoff theories to include the thickness stretching (normal strain) and transverse shear strain effects on the deformation of the structural element by virtue of the fact that, models of second-order expansions are analytically less complex as well as less computational demanding than models of the third and further higher-order expansions. The beam/plate/shell theories formulated on the second-order displacement models which accommodate the effect of the transverse shear but neglect the normal strain effect are called second-order shear deformation theories (SSDTs). Naghdi (1957) had utilized a second-order representation of the displacement model to present a suitable formulation of the stress – strain relations and appropriate boundary conditions associated with the small deflection theory of thin shells, which included the effects of the transverse normal and shear as well as rotary inertia on the shell deformation. These second-order displacement models which permitted the retention of the transverse normal and shear effects were also used by Pister and Westmann (1962) to develop a two dimensional elastostatic plate theory; Whitney and Sun (1973) to develop a laminated plate theory applicable to fibre reinforced composite materials under impact loading; Nelson and Lorch (1974) to model the static and dynamic response of laminated orthotropic plates. Khdeir and Reddy (1999) had studied the free vibrational response of laminated composite cross-ply and anti-symmetric angle-ply plates using the second-order shear deformation theory (SSDT). The work was reported to have close results to those of the FSDT and third-order shear deformation theory (TSDT) for the vibrational frequencies, albeit different from those of the classical shell theories for the case of thick laminates. However, for thin laminates all theories were reported to be in excellent agreement. The SSDT was also used by Shahrjerdi and Mustapha (2011) to analyze the free vibrational response of functionally graded quadrangle plates, the results revealed that the SSDT slightly over predict the natural frequencies. However, it was concluded that the results obtained were in good agreement with those of the TSDT and exact solutions. Shahrjerdi et al. (2010) had successfully applied the SSDT to the analysis of the stress distributions in solar functionally graded plates; the SSDT was shown to obtain acceptable results of the displacements and in-plane stresses when compared to other shear deformation theories available in literature. The effects of material compositions, temperature fields and geometry on the free vibration response of solar functionally graded plates was investigated by Shahrjerdi et al. (2011) using the SSDT. The results of the study were reported to be in considerable agreement with the HSDT. Szekrenyes (2013) utilized the SSDT in calculating the stress and energy release rates in delaminated orthotropic composite plates with symmetric lay-up and straight delamination front. The results were reported to have very good agreement with those of the 3D finite element model solution. Shahrjerdi et al. (2010), Shahrjerdi and Mustapha (2011), Shahrjerdi et al. (2011) and Szekrenyes (2013) had employed the polynomial second-order displacement model proposed by Khdeir and Reddy (1999) in their studies, the model permitted the accommodation of the transverse shear effect but neglected the thickness stretching effect. A detailed review of the displacement and stress based shear deformation theories of plates can be found in the work of Ghugal and Shimpi (2002), while a review of the shear deformation theories of laminated composite shells in application to buckling, flexure and dynamic responses can be found in the work of Reddy and Arciniega (2004).

This study is aimed at investigating the suitability of using the second-order shear deformation theory to analyze the static bending response of thin and moderately thick isotropic circular cylindrical shells. This is accomplished through the development of two second-order shear deformation theories formulated on two variant forms of the polynomial second-order displacement models already existing in literature. Results of the displacements and stresses generated from both second-order theories are compared to those of the classical shell theory, first and higher-order shear deformation theories in order to ascertain their efficacy in usage.

2 THEORETICAL FORMULATION OF THE SECOND-ORDER SHEAR DEFORMATION THEORIES (SSDTs)

The SSDTs developed in this study are based on a displacement approach and are formulated on two variant polynomial second-order displacement models which individually consist of seven (7) independent displacement parameters (u, v, w, ϕ_1, ϕ_2, ψ_1, ψ_2). These models account for an expansion of the surface displacements as quadratic functions of the thickness coordinate; together with a constant through thickness out-of-plane displacement component (deflection). The theoretical formulation of the present work is governed by the displacement field (also known as the displacement model), kinematics (strain–displacement relations) and material constitutive relations.

The assumptions of this study which dictate the choice of the displacement models are:

(1) The shell is moderately thick and falls within the order of approximations of Love first approximation shell theories $(h/R << 1;\quad (1+\alpha_3/R) \approx 1)$.

1. (2) The deformations of the shell are small.

(3) The shell thickness is considered small enough for the validity of the plane stress assumption $(\sigma_{33} = 0)$.

(4) The transverse normal does not stretch so that the normal strain is zero $(\varepsilon_{33} = 0)$.

2. (5) The transverse normals to the un-deformed reference surface no longer remain straight or normal after bending deformation.
3. (6) The elastic material is considered to be homogenous, isotropic and Hookean.

The assumption (1) permits the formulation of the present second-order shear deformation shell theories on the kinematic relations of linear elasticity, while assumption (5) represents the most significant deviation from Love theory and permits the retention of the transverse shear stresses and strains in the formulation of the governing equations of the fundamental shell element. The assumptions (2), (3), (4) and (5) of the present study had been found to be adequate for the study of the elastic deformation behavior of thin and moderately thick shells with radius of curvature to thickness ratios within $100 \geq R_i/h \geq 10$ (Amabili and Reddy, 2020; Viola et al., 2013).

Figure 1 refers to an isotropic doubly curved shell, where $(\alpha_1,\ \alpha_2)$ are curvilinear coordinate lines aligned with the shell reference surface $(\alpha_3 = 0)$. The thickness and principal radii of curvature are denoted by h and R_i (i = 1, 2) respectively. The thickness coordinate denoted by α_3 defines the distance of a point from the shell reference (middle) surface along the normal direction. The fundamental form of the reference surface as in Soedel (2004) is given as:

$$(ds)^2 = A^2 d\alpha_1^2 + B^2 d\alpha_2^2 \tag{2.1}$$

where the quantities A and B are the fundamental form parameters or Lame's parameters.

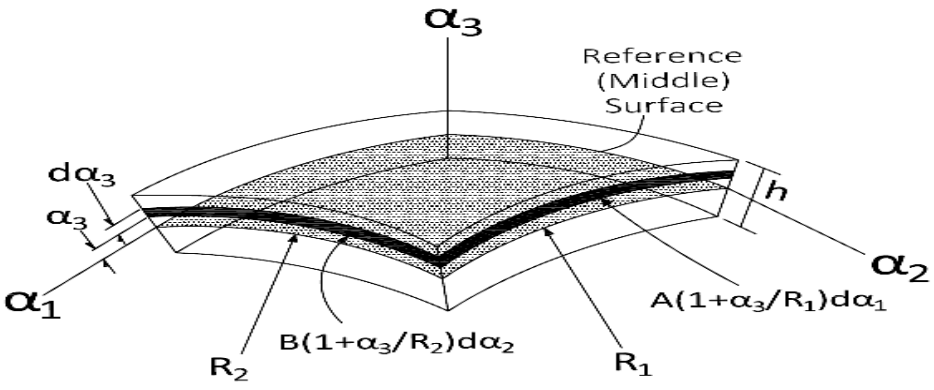

Figure 1 Differential element of a doubly curved shell

2.1 A SSDT based on the Displacement Field by Khdeir and Reddy

2.1.1 First Second-order Displacement Model – FSODM

The first second-order displacement model (FSODM) is assumed in the form by Khdeir and Reddy (1999) as:

$$\overline{U}(\alpha_1,\alpha_2,\alpha_3)=u+\alpha_3\varphi_1+\alpha_3{}^2\psi_1 \tag{2.2}$$

$$\overline{V}(\alpha_1,\alpha_2,\alpha_3)=v+\alpha_3\varphi_2+\alpha_3{}^2\psi_2 \tag{2.3}$$

$$\overline{W}(\alpha_1,\alpha_2,\alpha_3=0)=w \tag{2.4}$$

where ($\overline{U}$, $\overline{V}$, $\overline{W}$) are components of displacement of the 3D-shell element along the (α_1, α_2, α_3) directions. (u, v, w) represent displacements of a generic point (α_1, α_2, 0) on the reference surface of the shell in the (α_1, α_2, α_3) directions respectively. (φ_1, φ_2) are rotation of normals to the reference surface ($\alpha_3 = 0$) about the α_2 and α_1 directions. (ψ_1, ψ_2) are the second-order rotations.

2.1.2 Kinematic Relations and Strain Field

The equations of kinematics relating the strains (ε) and displacements for the 3D-shell element in linear elasticity (Viola et al., 2013) are given as:

$$\varepsilon_{11}=\frac{1}{1+\alpha_3/R_1}\left(\frac{1}{A}\frac{\partial\overline{U}}{\partial\alpha_1}+\frac{\overline{V}}{AB}\frac{\partial A}{\partial\alpha_2}+\frac{\overline{W}}{R_1}\right) \tag{2.5}$$

$$\varepsilon_{22}=\frac{1}{1+\alpha_3/R_2}\left(\frac{1}{B}\frac{\partial\overline{V}}{\partial\alpha_2}+\frac{\overline{U}}{AB}\frac{\partial B}{\partial\alpha_1}+\frac{\overline{W}}{R_2}\right) \tag{2.6}$$

$$\varepsilon_{12}=\frac{1}{1+\alpha_3/R_1}\left(\frac{1}{A}\frac{\partial\overline{V}}{\partial\alpha_1}-\frac{\overline{U}}{AB}\frac{\partial A}{\partial\alpha_2}\right)+\frac{1}{1+\alpha_3/R_2}\left(\frac{1}{B}\frac{\partial\overline{U}}{\partial\alpha_2}-\frac{\overline{V}}{AB}\frac{\partial B}{\partial\alpha_1}\right) \tag{2.7}$$

$$\varepsilon_{13}=\frac{1}{1+\alpha_3/R_1}\left(\frac{1}{A}\frac{\partial\overline{W}}{\partial\alpha_1}-\frac{\overline{U}}{R_1}\right)+\frac{\partial\overline{U}}{\partial\alpha_3} \tag{2.8}$$

$$\varepsilon_{23}=\frac{1}{1+\alpha_3/R_2}\left(\frac{1}{B}\frac{\partial\overline{W}}{\partial\alpha_2}-\frac{\overline{V}}{R_2}\right)+\frac{\partial\overline{V}}{\partial\alpha_3} \tag{2.9}$$

$$\varepsilon_{33}=\frac{\partial\overline{W}}{\partial\alpha_3} \tag{2.10}$$

Assumptions (1) and (4) permit the neglect of the term α_3/R_i (i = 1, 2) as well as the neglect of the through thickness stretching of the shell normal (normal strain effect, $\varepsilon_{33}=0$). The strain field associated with the shell element under consideration is obtained by the substitution of Eqs. (2.2) – (2.4) into Eqs. (2.5) – (2.9) as:

$$\begin{Bmatrix}\varepsilon_{11}\\ \varepsilon_{22}\\ \varepsilon_{12}\\ \varepsilon_{13}\\ \varepsilon_{23}\end{Bmatrix}=\begin{Bmatrix}\varepsilon_{11}{}^{(0)}\\ \varepsilon_{22}{}^{(0)}\\ \varepsilon_{12}{}^{(0)}\\ \varepsilon_{13}{}^{(0)}\\ \varepsilon_{23}{}^{(0)}\end{Bmatrix}+\alpha_3\begin{Bmatrix}\kappa_{11}{}^{(0)}\\ \kappa_{22}{}^{(0)}\\ \kappa_{12}{}^{(0)}\\ \kappa_{13}{}^{(0)}\\ \kappa_{23}{}^{(0)}\end{Bmatrix}+\alpha_3{}^2\begin{Bmatrix}\kappa_{11}{}^{(1)}\\ \kappa_{22}{}^{(1)}\\ \kappa_{12}{}^{(1)}\\ \kappa_{13}{}^{(1)}\\ \kappa_{23}{}^{(1)}\end{Bmatrix} \tag{2.11}$$

The components of strain expressed in generalized displacements (u, v, w, ϕ_1, ϕ_2, ψ_1, ψ_2) are obtained as:

$$\varepsilon_{11}^{(0)}=\frac{1}{A}\frac{\partial u}{\partial\alpha_1}+\frac{v}{AB}\frac{\partial A}{\partial\alpha_2}+\frac{w}{R_1};\quad \kappa_{11}^{(0)}=\frac{1}{A}\frac{\partial\varphi_1}{\partial\alpha_1}+\frac{\varphi_2}{AB}\frac{\partial A}{\partial\alpha_2};\quad \kappa_{11}^{(1)}=\frac{1}{A}\frac{\partial\psi_1}{\partial\alpha_1}+\frac{\psi_2}{AB}\frac{\partial A}{\partial\alpha_2};\quad \varepsilon_{22}^{(0)}=\frac{1}{B}\frac{\partial v}{\partial\alpha_2}+\frac{u}{AB}\frac{\partial B}{\partial\alpha_1}+\frac{w}{R_2};$$

$$\kappa_{22}^{(0)}=\frac{1}{B}\frac{\partial\varphi_2}{\partial\alpha_2}+\frac{\varphi_1}{AB}\frac{\partial B}{\partial\alpha_1};\ \kappa_{22}^{(1)}=\frac{1}{B}\frac{\partial\psi_2}{\partial\alpha_2}+\frac{\psi_1}{AB}\frac{\partial B}{\partial\alpha_1};\ \varepsilon_{12}^{(0)}=\frac{1}{A}\frac{\partial v}{\partial\alpha_1}-\frac{v}{AB}\frac{\partial B}{\partial\alpha_1}+\frac{1}{B}\frac{\partial u}{\partial\alpha_2}-\frac{u}{AB}\frac{\partial A}{\partial\alpha_2};$$

$$\kappa_{12}^{(0)}=\frac{1}{A}\frac{\partial\varphi_2}{\partial\alpha_1}-\frac{\varphi_2}{AB}\frac{\partial B}{\partial\alpha_1}+\frac{1}{B}\frac{\partial\varphi_1}{\partial\alpha_2}-\frac{\varphi_1}{AB}\frac{\partial A}{\partial\alpha_2};\ \kappa_{12}^{(1)}=\frac{1}{A}\frac{\partial\psi_2}{\partial\alpha_1}-\frac{\psi_2}{AB}\frac{\partial B}{\partial\alpha_1}+\frac{1}{B}\frac{\partial\psi_1}{\partial\alpha_2}-\frac{\psi_1}{AB}\frac{\partial A}{\partial\alpha_2};\ \varepsilon_{13}^{(0)}=\varphi_1+\frac{1}{A}\frac{\partial w}{\partial\alpha_1}-\frac{u}{R_1};$$

$$\kappa_{13}^{(0)}=2\psi_1;\ \kappa_{13}^{(1)}=-\frac{\psi_1}{R_1};\ \varepsilon_{23}^{(0)}=\varphi_2+\frac{1}{B}\frac{\partial w}{\partial\alpha_2}-\frac{v}{R_2};\ \kappa_{23}^{(0)}=2\psi_2;\ \kappa_{23}^{(1)}=-\frac{\psi_2}{R_2} \tag{2.12}$$

2.1.3 Stress – Strain Relations, Stress field and Stress Resultants

The material constitutive relations consistent with an isotropic material under plane stress assumption (Soedel, 2004) are given as:

$$\sigma_{11}=\frac{E}{1-\mu^2}\left(\varepsilon_{11}+\mu\varepsilon_{22}\right);\ \sigma_{22}=\frac{E}{1-\mu^2}\left(\varepsilon_{22}+\mu\varepsilon_{11}\right);\ \sigma_{12}=G\varepsilon_{12};\ \sigma_{13}=G\varepsilon_{13};\ \sigma_{23}=G\varepsilon_{23} \tag{2.13}$$

where (σ_{11},σ_{22}) are normal stresses, ($\sigma_{12},\sigma_{13},\sigma_{23}$) are shear stresses, μ is the poisons ratio, *E* is the elastic modulus and *G* is the modulus of rigidity expressed as $E/2(1+\mu)$. It should be noted that the shear stresses ($\sigma_{12}=\sigma_{21};\ \sigma_{13}=\sigma_{31};\ \sigma_{23}=\sigma_{32}$) are symmetric.

The stress – strain relations of the present theory are obtained by the substitution of Eq. (2.11) into the constitutive relations (Eq. (2.13)) as:

$$\sigma_{11}=\frac{E}{1-\mu^2}\left[\varepsilon_{11}^{(0)}+\mu\varepsilon_{22}^{(0)}+\alpha_3(\kappa_{11}^{(0)}+\mu\kappa_{22}^{(0)})+\alpha_3^2(\kappa_{11}^{(1)}+\mu\kappa_{22}^{(1)})\right] \tag{2.14}$$

$$\sigma_{22}=\frac{E}{1-\mu^2}\left[\varepsilon_{22}^{(0)}+\mu\varepsilon_{11}^{(0)}+\alpha_3(\kappa_{22}^{(0)}+\mu\kappa_{11}^{(0)})+\alpha_3^2(\kappa_{22}^{(1)}+\mu\kappa_{11}^{(1)})\right] \tag{2.15}$$

$$\sigma_{12}=\frac{E}{2(1+\mu)}\left[\varepsilon_{12}^{(0)}+\alpha_3\kappa_{12}^{(0)}+\alpha_3^2\kappa_{12}^{(1)}\right] \tag{2.16}$$

$$\sigma_{13}=\frac{E}{2(1+\mu)}\left[\varepsilon_{13}^{(0)}+\alpha_3\kappa_{13}^{(0)}+\alpha_3^2\kappa_{13}^{(1)}\right] \tag{2.17}$$

$$\sigma_{23}=\frac{E}{2(1+\mu)}\left[\varepsilon_{23}^{(0)}+\alpha_3\kappa_{23}^{(0)}+\alpha_3^2\kappa_{23}^{(1)}\right] \tag{2.18}$$

The stress resultants are defined as:

$$(N_{11},M_{11},L_{11})=\int_{-h/2}^{h/2}\sigma_{11}\left(1,\alpha_3,{\alpha_3}^2\right)d\alpha_3;\ (N_{12},M_{12},L_{12})=\int_{-h/2}^{h/2}\sigma_{12}\left(1,\alpha_3,{\alpha_3}^2\right)d\alpha_3;$$

$$(N_{22},M_{22},L_{22})=\int_{-h/2}^{h/2}\sigma_{22}\left(1,\alpha_3,{\alpha_3}^2\right)d\alpha_3;(Q_{13},R_{13},T_{13})=\int_{-h/2}^{h/2}\sigma_{13}\left(1,\alpha_3,{\alpha_3}^2\right)d\alpha_3;$$

$$(Q_{23}, R_{23}, T_{23}) = \int_{-h/2}^{h/2} \sigma_{23}\left(1, \alpha_3, {\alpha_3}^2\right) d\alpha_3 \tag{2.19}$$

where *N, M, L, Q, R, T* represent stress resultants.

By substituting Eqs. (2.14) – (2.18) into Eq. (2.19), we may then obtain the relationship between the stress resultants and strains as:

$$N_{11} = K({\varepsilon_{11}}^{(0)} + \mu {\varepsilon_{22}}^{(0)}) + D({\kappa_{11}}^{(1)} + \mu {\kappa_{22}}^{(1)});\ M_{11} = D({\kappa_{11}}^{(0)} + \mu {\kappa_{22}}^{(0)});\ L_{11} = D({\varepsilon_{11}}^{(0)} + \mu {\varepsilon_{22}}^{(0)}) + F({\kappa_{11}}^{(1)} + \mu {\kappa_{22}}^{(1)});$$

$$N_{22} = K({\varepsilon_{22}}^{(0)} + \mu {\varepsilon_{11}}^{(0)}) + D({\kappa_{22}}^{(1)} + \mu {\kappa_{11}}^{(1)}); \quad M_{22} = D({\kappa_{22}}^{(0)} + \mu {\kappa_{11}}^{(0)}); \quad L_{22} = D({\varepsilon_{22}}^{(0)} + \mu {\varepsilon_{11}}^{(0)}) + F({\kappa_{22}}^{(1)} + \mu {\kappa_{11}}^{(1)});$$

$$N_{12} = \frac{K(1-\mu)}{2}{\varepsilon_{12}}^{(0)} + \frac{D(1-\mu)}{2}{\kappa_{12}}^{(1)};\ M_{12} = \frac{D(1-\mu)}{2}{\kappa_{12}}^{(0)};\ L_{12} = \frac{D(1-\mu)}{2}{\varepsilon_{12}}^{(0)} + \frac{F(1-\mu)}{2}{\kappa_{12}}^{(1)}; \tag{2.20}$$

$$Q_{13} = \frac{K(1-\mu)}{2}{\varepsilon_{13}}^{(0)} + \frac{D(1-\mu)}{2}{\kappa_{13}}^{(1)};\ R_{13} = \frac{D(1-\mu)}{2}{\kappa_{13}}^{(0)};\ T_{13} = \frac{D(1-\mu)}{2}{\varepsilon_{13}}^{(0)} + \frac{F(1-\mu)}{2}{\kappa_{13}}^{(1)};$$

$$Q_{23} = \frac{K(1-\mu)}{2}{\varepsilon_{23}}^{(0)} + \frac{D(1-\mu)}{2}{\kappa_{23}}^{(1)};\ R_{23} = \frac{D(1-\mu)}{2}{\kappa_{23}}^{(0)};\ T_{23} = \frac{D(1-\mu)}{2}{\varepsilon_{23}}^{(0)} + \frac{F(1-\mu)}{2}{\kappa_{23}}^{(1)}$$

where *K*, *D* and *F* are the shell stiffnesses obtained as:

$$(K, D, F) = \frac{E}{1-\mu^2}\left(h, \frac{h^3}{12}, \frac{h^5}{80}\right) \tag{2.21}$$

2.1.4 Stress – Stress Resultant Relations

Solving Eq. (2.20) for the strains, the stresses (Eqs. (2.14) – (2.18)) are obtained in terms of stress resultants as:

$$\sigma_{11} = \frac{E}{1-\mu^2}\left\{\frac{N_{11}}{K} - \frac{D}{K}\left[\frac{L_{11}K - N_{11}D}{FK - D^2}\right] + \alpha_3\frac{M_{11}}{D} + \alpha_3^2\left(\frac{L_{11}K - N_{11}D}{FK - D^2}\right)\right\} \tag{2.22}$$

$$\sigma_{22} = \frac{E}{1-\mu^2}\left\{\frac{N_{22}}{K} - \frac{D}{K}\left[\frac{L_{22}K - N_{22}D}{FK - D^2}\right] + \alpha_3\frac{M_{22}}{D} + \alpha_3^2\left(\frac{L_{22}K - N_{22}D}{FK - D^2}\right)\right\} \tag{2.23}$$

$$\sigma_{12} = \frac{E}{1+\mu}\left\{\frac{N_{12}}{K(1-\mu)} - \frac{D}{K}\left(\frac{L_{12}K - N_{12}D}{(FK - D^2)(1-\mu)}\right) + \alpha_3\left[\frac{M_{12}}{D(1-\mu)}\right] + \alpha_3^2\left[\frac{L_{12}K - N_{12}D}{(FK - D^2)(1-\mu)}\right]\right\} \tag{2.24}$$

$$\sigma_{13} = \frac{E}{1+\mu}\left\{\frac{Q_{13}}{K(1-\mu)} - \frac{D}{K}\left(\frac{T_{13}K - Q_{13}D}{(FK - D^2)(1-\mu)}\right) + \alpha_3\left[\frac{R_{13}}{D(1-\mu)}\right] + \alpha_3^2\left[\frac{T_{13}K - Q_{13}D}{(FK - D^2)(1-\mu)}\right]\right\} \tag{2.25}$$

$$\sigma_{23} = \frac{E}{1+\mu}\left\{\frac{Q_{23}}{K(1-\mu)} - \frac{D}{K}\left(\frac{T_{23}K - Q_{23}D}{(FK - D^2)(1-\mu)}\right) + \alpha_3\left[\frac{R_{23}}{D(1-\mu)}\right] + \alpha_3^2\left[\frac{T_{23}K - Q_{23}D}{(FK - D^2)(1-\mu)}\right]\right\} \tag{2.26}$$

2.1.5 Equations of Static Equilibrium

We now utilize the principle of virtual work to derive the equations of equilibrium appropriate to the displacement field (Eqs. (2.2) – (2.4)). The principle of virtual work is expressed mathematically (Reddy and Arciniega, 2004) as:

$$\delta w = \delta w_I + \delta w_E = 0 \tag{2.27}$$

where the virtual work due to internal forces is given as:

$$\delta w_I = \int_{\alpha_1}\int_{\alpha_2}\int_{\alpha_3}\left(\sigma_{11}\delta\varepsilon_{11}+\sigma_{22}\delta\varepsilon_{22}+\sigma_{12}\delta\varepsilon_{12}+\sigma_{13}\delta\varepsilon_{13}+\sigma_{23}\delta\varepsilon_{23}\right)AB d\alpha_1 d\alpha_2 d\alpha_3 \tag{2.28}$$

while the virtual work due to external forces is given as:

$$\delta w_E = -\int_{\alpha_1}\int_{\alpha_2}\left(q_1\delta u + q_2\delta v + q_3\delta w\right)AB\, d\alpha_1 d\alpha_2 \tag{2.29}$$

q_1, q_2 and q_3 are the distributed load terms.

The principle of virtual work when applied to the present FSODM theory results in:

$$\begin{aligned} 0 &= \int_{\alpha_1}\int_{\alpha_2}\left[\int_{-h/2}^{h/2}\left(\sigma_{11}\delta\varepsilon_{11}+\sigma_{22}\delta\varepsilon_{22}+\sigma_{12}\delta\varepsilon_{12}+\sigma_{13}\delta\varepsilon_{13}+\sigma_{23}\delta\varepsilon_{23}\right)d\alpha_3 - \left(q_1\delta u + q_2\delta v + q_3\delta w\right)\right]AB d\alpha_1 d\alpha_2 \\ &= \int_{\alpha_1}\int_{\alpha_2}\Big[N_{11}\delta\varepsilon_{11}^{(0)} + M_{11}\delta\kappa_{11}^{(0)} + L_{11}\delta\kappa_{11}^{(1)} + N_{22}\delta\varepsilon_{22}^{(0)} + M_{22}\delta\kappa_{22}^{(0)} + L_{22}\delta\kappa_{22}^{(1)} + N_{12}\delta\varepsilon_{12}^{(0)} + M_{12}\delta\kappa_{12}^{(0)} \\ &+ L_{12}\delta\kappa_{12}^{(1)} + Q_{13}\delta\varepsilon_{13}^{(0)} + R_{13}\delta\kappa_{13}^{(0)} + T_{13}\delta\kappa_{13}^{(1)} + Q_{23}\delta\varepsilon_{23}^{(0)} + R_{23}\delta\kappa_{23}^{(0)} + T_{23}\delta\kappa_{23}^{(1)} - q_1\delta u - q_2\delta v - q_3\delta w\Big]AB d\alpha_1 d\alpha_2 \end{aligned} \tag{2.30}$$

Substituting the strains (Eq. (2.12)) into Eq. (2.30) and integrating by parts the displacement gradients, the equations of equilibrium are obtained by the vanishing of the coefficients of variations δu , δv , δw , $\delta\varphi_1$, $\delta\varphi_2$, $\delta\psi_1$ and $\delta\psi_2$ as:

$$\delta u: \frac{\partial\left(N_{11}B\right)}{\partial\alpha_1} - N_{22}\frac{\partial B}{\partial\alpha_1} + \frac{\partial\left(N_{21}A\right)}{\partial\alpha_2} + N_{12}\frac{\partial A}{\partial\alpha_2} + Q_{13}\frac{AB}{R_1} + q_1 AB = 0 \tag{2.31}$$

$$\delta v: \frac{\partial\left(N_{22}A\right)}{\partial\alpha_2} - N_{11}\frac{\partial A}{\partial\alpha_2} + \frac{\partial\left(N_{12}B\right)}{\partial\alpha_1} + N_{21}\frac{\partial B}{\partial\alpha_1} + Q_{23}\frac{AB}{R_2} + q_2 AB = 0 \tag{2.32}$$

$$\delta w: \frac{\partial\left(Q_{13}B\right)}{\partial\alpha_1} + \frac{\partial\left(Q_{23}A\right)}{\partial\alpha_2} - \left(\frac{N_{11}}{R_1} + \frac{N_{22}}{R_2}\right) + q_3 AB = 0 \tag{2.33}$$

$$\delta\varphi_1: \frac{\partial\left(M_{11}B\right)}{\partial\alpha_1} - M_{22}\frac{\partial B}{\partial\alpha_1} + \frac{\partial\left(M_{21}A\right)}{\partial\alpha_2} + M_{12}\frac{\partial A}{\partial\alpha_2} - Q_{13}AB = 0 \tag{2.34}$$

$$\delta\varphi_2: \frac{\partial\left(M_{22}A\right)}{\partial\alpha_2} - M_{11}\frac{\partial A}{\partial\alpha_2} + \frac{\partial\left(M_{12}B\right)}{\partial\alpha_1} + M_{21}\frac{\partial B}{\partial\alpha_1} - Q_{23}AB = 0 \tag{2.35}$$

$$\delta\psi_1: \frac{\partial\left(L_{11}B\right)}{\partial\alpha_1} - L_{22}\frac{\partial B}{\partial\alpha_1} + \frac{\partial\left(L_{21}A\right)}{\partial\alpha_2} + L_{12}\frac{\partial A}{\partial\alpha_2} - 2R_{13}AB + T_{13}\frac{AB}{R_1} = 0 \tag{2.36}$$

$$\delta\psi_2: \frac{\partial\left(L_{22}A\right)}{\partial\alpha_2} - L_{11}\frac{\partial A}{\partial\alpha_2} + \frac{\partial\left(L_{12}B\right)}{\partial\alpha_1} + L_{21}\frac{\partial B}{\partial\alpha_1} - 2R_{23}AB + T_{23}\frac{AB}{R_2} = 0 \tag{2.37}$$

It should be noted that from the above equilibrium equations (Eqs. (2.31) – (2.37)), if Eqs. (2.36) and (2.37) introduced by $\delta\psi_1, \delta\psi_2$ are taken to be zero. The equations of equilibrium would then reduce to Love's equilibrium equations as in Soedel (2004).

2.1.6 Application of the Theory based on the FSODM to Circular Cylindrical Shells of Revolution

The derived governing equations of the moderately thick shell element associated with the FSODM theory are now applied to the particular case of circular cylindrical shells (See Figure 2).

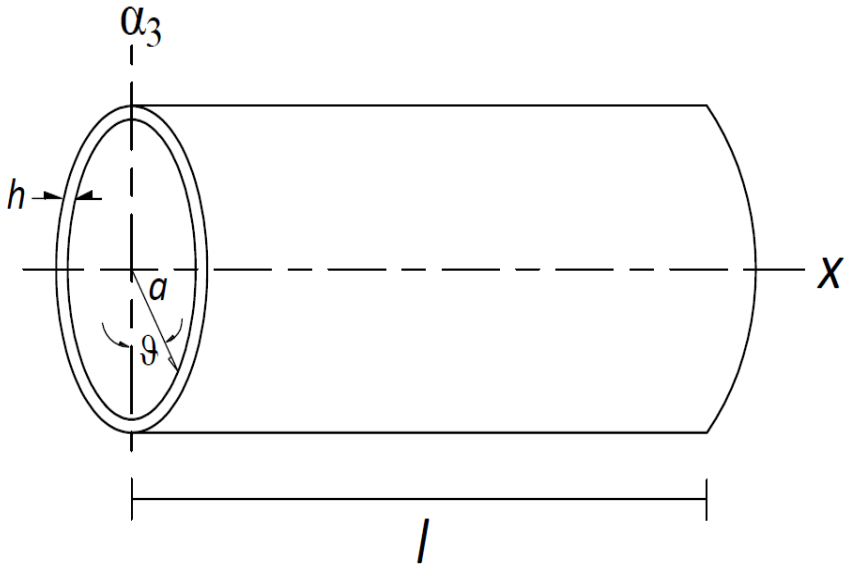

Figure 2 A circular cylindrical shell

The fundamental form of the reference surface (Soedel, 2004) is given as:

$$(ds)^2 = (dx)^2 + a^2(d\vartheta)^2 \tag{2.38}$$

The Lame parameters are gotten by the comparison of Eq. (2.38) and Eq. (1) as:

$$A = 1,\ B = a = const. \tag{2.39}$$

On account of the circular cylindrical shell being of single curvature, the surface parameters are obtained as:

$$\alpha_1 = x,\ \alpha_2 = \vartheta,\ R_1 = R_x = \infty,\ R_2 = R_\vartheta = a = const.,\ 1/R_x = 0 \tag{2.40}$$

where a is defined as the constant radius of the circular cylindrical shell and the subscripts 1,2,3 are now replaced by x, ϑ and z respectively.

In order to obtain the differential equations of static equilibrium for the circular cylindrical shell element, Eqs. (2.39) and (2.40) are substituted into Eqs. (2.31) – (2.37) to obtain:

$$\frac{\partial N_{xx}}{\partial x} + \frac{1}{a}\frac{\partial N_{\vartheta x}}{\partial \vartheta} + q_x = 0 \tag{2.41}$$

$$\frac{\partial N_{x\vartheta}}{\partial x} + \frac{1}{a}\frac{\partial N_{\vartheta\vartheta}}{\partial \vartheta} + \frac{Q_{\vartheta z}}{a} + q_\vartheta = 0 \tag{2.42}$$

$$\frac{\partial Q_{xz}}{\partial x} + \frac{1}{a}\frac{\partial Q_{\vartheta z}}{\partial \vartheta} - \frac{N_{\vartheta\vartheta}}{a} + q_z = 0 \tag{2.43}$$

$$\frac{\partial M_{xx}}{\partial x} + \frac{1}{a}\frac{\partial M_{\vartheta x}}{\partial \vartheta} - Q_{xz} = 0 \tag{2.44}$$

$$\frac{\partial M_{x\vartheta}}{\partial x}+\frac{1}{a}\frac{\partial M_{\vartheta\vartheta}}{\partial \vartheta}-Q_{\vartheta z}=0 \tag{2.45}$$

$$\frac{\partial L_{xx}}{\partial x}+\frac{1}{a}\frac{\partial L_{\vartheta x}}{\partial \vartheta}-2R_{xz}=0 \tag{2.46}$$

$$\frac{\partial L_{x\vartheta}}{\partial x}+\frac{1}{a}\frac{\partial L_{\vartheta\vartheta}}{\partial \vartheta}-2R_{\vartheta z}+\frac{T_{\vartheta z}}{a}=0 \tag{2.47}$$

The components of strain for the circular cylindrical shell are obtained by substituting Eqs. (2.39) and (2.40) into Eq. (2.12) as:

$$\varepsilon_{xx}^{(0)}=\frac{\partial u}{\partial x};\ \kappa_{xx}^{(0)}=\frac{\partial \varphi_x}{\partial x};\ \kappa_{xx}^{(1)}=\frac{\partial \psi_x}{\partial x};\ \varepsilon_{\vartheta\vartheta}^{(0)}=\frac{1}{a}\left(\frac{\partial v}{\partial \vartheta}+w\right);\ \kappa_{\vartheta\vartheta}^{(0)}=\frac{1}{a}\frac{\partial \varphi_\vartheta}{\partial \vartheta};\ \kappa_{\vartheta\vartheta}^{(1)}=\frac{1}{a}\frac{\partial \psi_\vartheta}{\partial \vartheta};$$

$$\varepsilon_{x\vartheta}^{(0)}=\frac{1}{a}\frac{\partial u}{\partial \vartheta}+\frac{\partial v}{\partial x};\ \kappa_{x\vartheta}^{(0)}=\frac{1}{a}\frac{\partial \varphi_x}{\partial \vartheta}+\frac{\partial \varphi_\vartheta}{\partial x};\ \kappa_{x\vartheta}^{(1)}=\frac{1}{a}\frac{\partial \psi_x}{\partial \vartheta}+\frac{\partial \psi_\vartheta}{\partial x};\ \varepsilon_{xz}^{(0)}=\varphi_x+\frac{\partial w}{\partial x};\ \kappa_{xz}^{(0)}=2\psi_x;$$

$$\kappa_{xz}^{(1)}=0;\ \varepsilon_{\vartheta z}^{(0)}=\varphi_\vartheta+\frac{1}{a}\frac{\partial w}{\partial \vartheta}-\frac{v}{a};\ \kappa_{\vartheta z}^{(0)}=2\psi_\vartheta;\ \kappa_{\vartheta z}^{(1)}=-\frac{\psi_\vartheta}{a} \tag{2.48}$$

The stress resultant – displacement relations are obtained by the substitution of Eq. (2.48) into Eq. (2.20) as:

$$N_{xx}=K\left[\frac{\partial u}{\partial x}+\frac{\mu}{a}\left(\frac{\partial v}{\partial \vartheta}+w\right)\right]+D\left[\frac{\partial \psi_x}{\partial x}+\frac{\mu}{a}\frac{\partial \psi_\vartheta}{\partial \vartheta}\right];\ M_{xx}=D\left[\frac{\partial \varphi_x}{\partial x}+\frac{\mu}{a}\frac{\partial \varphi_\vartheta}{\partial \vartheta}\right];$$

$$L_{xx}=D\left[\frac{\partial u}{\partial x}+\frac{\mu}{a}\left(\frac{\partial v}{\partial \vartheta}+w\right)\right]+F\left[\frac{\partial \psi_x}{\partial x}+\frac{\mu}{a}\frac{\partial \psi_\vartheta}{\partial \vartheta}\right] \tag{2.49}$$

$$N_{\vartheta\vartheta}=K\left[\mu\frac{\partial u}{\partial x}+\frac{1}{a}\left(\frac{\partial v}{\partial \vartheta}+w\right)\right]+D\left[\mu\frac{\partial \psi_x}{\partial x}+\frac{1}{a}\frac{\partial \psi_\vartheta}{\partial \vartheta}\right];\ M_{\vartheta\vartheta}=D\left[\mu\frac{\partial \varphi_x}{\partial x}+\frac{1}{a}\frac{\partial \varphi_\vartheta}{\partial \vartheta}\right];$$

$$L_{\vartheta\vartheta}=D\left[\mu\frac{\partial u}{\partial x}+\frac{1}{a}\left(\frac{\partial v}{\partial \vartheta}+w\right)\right]+F\left[\mu\frac{\partial \psi_x}{\partial x}+\frac{1}{a}\frac{\partial \psi_\vartheta}{\partial \vartheta}\right] \tag{2.50}$$

$$N_{x\vartheta}=\frac{K(1-\mu)}{2}\left[\frac{1}{a}\frac{\partial u}{\partial \vartheta}+\frac{\partial v}{\partial x}\right]+\frac{D(1-\mu)}{2}\left[\frac{\partial \psi_\vartheta}{\partial x}+\frac{1}{a}\frac{\partial \psi_x}{\partial \vartheta}\right];\ M_{x\vartheta}=\frac{D(1-\mu)}{2}\left[\frac{\partial \varphi_\vartheta}{\partial x}+\frac{1}{a}\frac{\partial \varphi_x}{\partial \vartheta}\right];$$

$$L_{x\vartheta}=\frac{D(1-\mu)}{2}\left[\frac{1}{a}\frac{\partial u}{\partial \vartheta}+\frac{\partial v}{\partial x}\right]+\frac{F(1-\mu)}{2}\left[\frac{\partial \psi_\vartheta}{\partial x}+\frac{1}{a}\frac{\partial \psi_x}{\partial \vartheta}\right] \tag{2.51}$$

$$Q_{xz}=\frac{K(1-\mu)}{2}\left[\frac{\partial w}{\partial x}+\varphi_x\right];\ R_{xz}=D(1-\mu)\psi_x;\ T_{xz}=\frac{D(1-\mu)}{2}\left[\frac{\partial w}{\partial x}+\varphi_x\right] \tag{2.52}$$

$$Q_{\vartheta z}=\frac{K(1-\mu)}{2}\left[\frac{1}{a}\frac{\partial w}{\partial \vartheta}+\varphi_\vartheta-\frac{v}{a}\right]-\frac{D(1-\mu)}{2}\left[\frac{\psi_\vartheta}{a}\right];\ R_{\vartheta z}=D(1-\mu)\psi_\vartheta;$$

$$T_{\vartheta z}=\frac{D(1-\mu)}{2}\left[\varphi_{\vartheta}+\frac{1}{a}\frac{\partial w}{\partial\vartheta}-\frac{v}{a}\right]-\frac{F(1-\mu)}{2}\left[\frac{\psi_{\vartheta}}{a}\right] \tag{2.53}$$

The equilibrium equations are expressed in terms of the generalized displacement components (u, v, w, φ_x, φ_ϑ, ψ_x and ψ_ϑ) by the substitution of the stress resultant – displacement relations (Eqs. (2.49) – (2.53)) into Eqs. (2.41) – (2.47) as:

$$\frac{\partial^2 u}{\partial x^2}+\left(\frac{1-\mu}{2a^2}\right)\frac{\partial^2 u}{\partial\vartheta^2}+\left(\frac{1+\mu}{2a}\right)\frac{\partial^2 v}{\partial\vartheta\partial x}+\frac{\mu}{a}\frac{\partial w}{\partial x}+\frac{h^2}{12}\frac{\partial^2\psi_x}{\partial x^2}+\frac{h^2}{12}\left(\frac{1-\mu}{2a^2}\right)\frac{\partial^2\psi_x}{\partial\vartheta^2}+\frac{h^2}{12}\left(\frac{1+\mu}{2a}\right)\frac{\partial^2\psi_\vartheta}{\partial\vartheta\partial x}=-\frac{q_x(1-\mu^2)}{Eh} \tag{2.54}$$

$$\begin{aligned}&\frac{\partial^2 u}{\partial x\partial\vartheta}\left(\frac{1+\mu}{2a}\right)+\left(\frac{1-\mu}{2}\right)\frac{\partial^2 v}{\partial x^2}+\frac{1}{a^2}\frac{\partial^2 v}{\partial\vartheta^2}+\left(\frac{3-\mu}{2a^2}\right)\frac{\partial w}{\partial\vartheta}+\frac{h^2}{24}(1-\mu)\frac{\partial^2\psi_\vartheta}{\partial x^2}+\frac{h^2}{12}\left(\frac{1+\mu}{2a}\right)\frac{\partial^2\psi_x}{\partial x\partial\vartheta}+\frac{h^2}{12a^2}\frac{\partial^2\psi_\vartheta}{\partial\vartheta^2}\\&-\left(\frac{1-\mu}{2a^2}\right)v-\frac{h^2}{12}\left(\frac{1-\mu}{2a^2}\right)\psi_\vartheta+\left(\frac{1-\mu}{2a}\right)\varphi_\vartheta=-\frac{q_\vartheta(1-\mu^2)}{Eh}\end{aligned} \tag{2.55}$$

$$\begin{aligned}&\left(\frac{1-\mu}{2}\right)\frac{\partial^2 w}{\partial x^2}+\left(\frac{1-\mu}{2}\right)\frac{\partial\varphi_x}{\partial x}+\left(\frac{1-\mu}{2a^2}\right)\frac{\partial^2 w}{\partial\vartheta^2}+\left(\frac{1-\mu}{2a}\right)\frac{\partial\varphi_\vartheta}{\partial\vartheta}-\left(\frac{3-\mu}{2a^2}\right)\frac{\partial v}{\partial\vartheta}-\frac{w}{a^2}-\frac{\mu}{a}\frac{\partial u}{\partial x}-\frac{h^2}{12}\frac{\mu}{a}\frac{\partial\psi_x}{\partial x}\\&-\frac{h^2}{12}\left(\frac{3-\mu}{2a^2}\right)\frac{\partial\psi_\vartheta}{\partial\vartheta}=-\frac{q_z(1-\mu^2)}{Eh}\end{aligned} \tag{2.56}$$

$$\frac{h^2}{12}\frac{\partial^2\varphi_x}{\partial x^2}+\frac{h^2}{12}\left(\frac{1-\mu}{2a^2}\right)\frac{\partial^2\varphi_x}{\partial\vartheta^2}-\frac{1-\mu}{2}\left(\varphi_x+\frac{\partial w}{\partial x}\right)+\frac{h^2}{12}\left(\frac{1+\mu}{2a}\right)\frac{\partial^2\varphi_\vartheta}{\partial\vartheta\partial x}=0 \tag{2.57}$$

$$\frac{h^2(1-\mu)}{24}\left(\frac{\partial^2\varphi_\vartheta}{\partial x^2}+\frac{\psi_\vartheta}{a}\right)+\frac{h^2}{12a^2}\frac{\partial^2\varphi_\vartheta}{\partial\vartheta^2}-\frac{1-\mu}{2}\left(\varphi_\vartheta+\frac{\partial w}{\partial\vartheta}\frac{1}{a}-\frac{v}{a}\right)+\frac{h^2}{12}\left(\frac{1+\mu}{2a}\right)\frac{\partial^2\varphi_x}{\partial\vartheta\partial x}=0 \tag{2.58}$$

$$\begin{aligned}&\frac{h^2}{12}\left(\frac{\partial^2 u}{\partial x^2}+\frac{\mu}{a}\frac{\partial w}{\partial x}\right)+\frac{h^2}{80}\frac{\partial^2\psi_x}{\partial x^2}+\frac{h^2}{12}\left(\frac{1-\mu}{2a^2}\right)\frac{\partial^2 u}{\partial\vartheta^2}+\frac{h^2(1-\mu)}{160a^2}\frac{\partial^2\psi_x}{\partial\vartheta^2}-\frac{h^2(1-\mu)}{6}\psi_x+\frac{h^2}{12}\left(\frac{1+\mu}{2a}\right)\frac{\partial^2 v}{\partial\vartheta\partial x}\\&+\frac{h^2}{80}\left(\frac{1+\mu}{2a}\right)\frac{\partial^2\psi_\vartheta}{\partial\vartheta\partial x}=0\end{aligned} \tag{2.59}$$

$$\begin{aligned}&\frac{h^2}{12}\left(\frac{1+\mu}{2a}\right)\frac{\partial^2 u}{\partial x\partial\vartheta}+\frac{h^2(1-\mu)}{24}\frac{\partial^2 v}{\partial x^2}+\frac{h^2(1-\mu)}{160}\frac{\partial^2\psi_\vartheta}{\partial x^2}+\frac{h^2}{80}\left(\frac{1+\mu}{2a}\right)\frac{\partial^2\psi_x}{\partial x\partial\vartheta}+\frac{h^2}{12}\left(\frac{3-\mu}{2a^2}\right)\frac{\partial w}{\partial\vartheta}\\&-h^2(1-\mu)\psi_\vartheta\left(\frac{1}{6}+\frac{1}{160a^2}\right)+\frac{h^2}{12a^2}\frac{\partial^2 v}{\partial\vartheta^2}+\frac{h^2}{80a^2}\frac{\partial^2\psi_\vartheta}{\partial\vartheta^2}+\frac{h^2(1-\mu)}{24a}\varphi_\vartheta-\frac{h^2(1-\mu)}{24a^2}v=0\end{aligned} \tag{2.60}$$

2.2 A SSDT based on a Truncated Form of the Unconstrained Third-order Displacement Field by Reddy and Liu

2.2.1 Second Second-order Displacement Model – SSODM

The second second-order displacement model (SSODM) is a truncated form to the second-order of the unconstrained third-order displacement model proposed by Reddy and Liu (1985), taken as:

$$\overline{U}(\alpha_1,\alpha_2,\alpha_3)=u\left(1+\frac{\alpha_3}{R_1}\right)+\alpha_3\varphi_1+{\alpha_3}^2\psi_1 \tag{2.61}$$

$$\overline{V}(\alpha_1,\alpha_2,\alpha_3)=v\left(1+\frac{\alpha_3}{R_2}\right)+\alpha_3\varphi_2+{\alpha_3}^2\psi_2 \tag{2.62}$$

$$\overline{W}(\alpha_1,\alpha_2,\alpha_3=0)=w \tag{2.63}$$

where R_1 and R_2 are the radii of curvature of the mid-surface.

The modification of the first displacement field/model (Eqs. (2.2) and (2.3)) by the terms $1+\alpha_3/R_i$ (i = 1, 2) as seen in Eqs. (2.61) and (2.62) is to accommodate the initial curvature of the shell's cross section. However, this has no effect on the expressions of the strain components related to the in-plane normal and shear strains ($\varepsilon_{11},\varepsilon_{22},\varepsilon_{12}$) due to the assumption of the terms $\alpha_3/R_i<<1$ as being negligible.

2.2.2 Strain – Displacement Relations

The kinematic relations for the in-plane normal and shear strains $\varepsilon_{11},\varepsilon_{22},\varepsilon_{12}$ are given as Eqs. (2.5) – (2.7). However, the expressions of the transverse shear strain – displacements relations consistent with the adopted displacement field (Eqs. (2.61) – (2.63)) for an elemental shell are given by Reddy and Liu (1985) as:

$$\varepsilon_{13}=\frac{1}{A}\frac{\partial\overline{W}}{\partial\alpha_1}-\frac{u}{R_1}+\frac{\partial\overline{U}}{\partial\alpha_3};\ \varepsilon_{23}=\frac{1}{B}\frac{\partial\overline{W}}{\partial\alpha_2}-\frac{v}{R_2}+\frac{\partial\overline{V}}{\partial\alpha_3} \tag{2.64}$$

2.2.3 Strain Field

The displacement field (Eqs. (2.61) – (2.63)) are introduced into the strain – displacement relations (Eqs. (2.5) – (2.7) and Eq. (2.64)) in order to obtain the corresponding strain field for the present SSODM theory as:

$$\begin{Bmatrix}\varepsilon_{11}\\ \varepsilon_{22}\\ \varepsilon_{12}\end{Bmatrix}=\begin{Bmatrix}\varepsilon_{11}^{(0)}\\ \varepsilon_{22}^{(0)}\\ \varepsilon_{12}^{(0)}\end{Bmatrix}+\alpha_3\begin{Bmatrix}\kappa_{11}^{(0)}\\ \kappa_{22}^{(0)}\\ \kappa_{12}^{(0)}\end{Bmatrix}+\alpha_3^2\begin{Bmatrix}\kappa_{11}^{(1)}\\ \kappa_{22}^{(1)}\\ \kappa_{12}^{(1)}\end{Bmatrix} \tag{2.65}$$

$$\begin{Bmatrix}\varepsilon_{13}\\ \varepsilon_{23}\end{Bmatrix}=\begin{Bmatrix}\varepsilon_{13}^{(0)}\\ \varepsilon_{23}^{(0)}\end{Bmatrix}+\alpha_3\begin{Bmatrix}\kappa_{13}^{(0)}\\ \kappa_{23}^{(0)}\end{Bmatrix} \tag{2.66}$$

where the expressions of the in-plane normal and shear strain components $\varepsilon_{11}^{(0)},\kappa_{11}^{(0)},\kappa_{11}^{(1)},\varepsilon_{22}^{(0)},\kappa_{22}^{(0)},\kappa_{22}^{(1)},\varepsilon_{12}^{(0)},\kappa_{12}^{(0)}$ and $\kappa_{12}^{(1)}$ remain unmodified and are obtained in terms of displacement components as given in Eq. (2.12).

The transverse shear strain components are now obtained as:

$${\varepsilon_{13}}^{(0)}=\varphi_1+\frac{1}{A}\frac{\partial w}{\partial\alpha_1};\ {\kappa_{13}}^{(0)}=2\psi_1;\ {\varepsilon_{23}}^{(0)}=\varphi_2+\frac{1}{B}\frac{\partial w}{\partial\alpha_2};\ {\kappa_{23}}^{(0)}=2\psi_2 \tag{2.67}$$

2.2.4 Stress Field, Stress Resultants and Stress – Stress Resultant Relations

The in-plane normal and shear stresses $\sigma_{11},\sigma_{22},\sigma_{12}$ are gotten by the substitution of Eq. (2.65) into their corresponding stress – strain laws (refer to Eq. (2.13)). This also results in the same expressions as given in Eqs. (2.14) – (2.16).

The transverse shear stresses in this case are now obtained by the substitution of Eq. (2.66) into the stress – strain laws for the transverse shear (see Eq. (2.13)) as:

$$\sigma_{13}=\frac{E}{2(1+\mu)}\left[\varepsilon_{13}^{(0)}+\alpha_3\kappa_{13}^{(0)}\right];\ \sigma_{23}=\frac{E}{2(1+\mu)}\left[\varepsilon_{23}^{(0)}+\alpha_3\kappa_{23}^{(0)}\right] \tag{2.68}$$

The stress resultants are now defined as:

$$(N_{11},N_{22},N_{12},Q_{13},Q_{23})=\int_{-h/2}^{h/2}(\sigma_{11},\sigma_{22},\sigma_{12},\sigma_{13},\sigma_{23})\,d\alpha_3 \tag{2.69}$$

$$(M_{11},M_{22},M_{12},R_{13},R_{23})=\int_{-h/2}^{h/2}(\sigma_{11},\sigma_{22},\sigma_{12},\sigma_{13},\sigma_{23})\,\alpha_3\,d\alpha_3 \tag{2.70}$$

$$(L_{11},L_{22},L_{12})=\int_{-h/2}^{h/2}(\sigma_{11},\sigma_{22},\sigma_{12})\,\alpha_3^2\,d\alpha_3 \tag{2.71}$$

The substitution of Eqs. ((2.14) – (2.16) and (2.68)) into Eqs. (2.69) – (2.71) results in expressions of the stress resultants in terms of strain components for the SSODM theory. The equations of the stress resultants N_{11}, N_{22}, N_{12}, M_{11}, M_{22}, M_{12}, L_{11}, L_{22} and L_{12} expressed in strain components also remain unmodified and are as given in Eq. (2.20).

The stress resultants associated with the transverse shear stresses are now obtained as:

$$Q_{13}=\frac{K(1-\mu)}{2}\varepsilon_{13}^{(0)};\ Q_{23}=\frac{K(1-\mu)}{2}\varepsilon_{23}^{(0)};\ R_{13}=\frac{D(1-\mu)}{2}\kappa_{13}^{(0)};\ R_{23}=\frac{D(1-\mu)}{2}\kappa_{23}^{(0)} \tag{2.72}$$

The expressions for the stress – stress resultant relations for the in-plane normal and shear stresses remain unmodified and are as given in Eqs. (2.22) – (2.24).

The stress – stress resultant relations associated with the transverse shear stresses are obtained by solving Eq. (2.72) for the strain components and substituting the resulting expressions into Eq. (2.68) to obtain:

$$\sigma_{13}=\frac{E}{1+\mu}\left\{\frac{Q_{13}}{K(1-\mu)}+\alpha_3\frac{R_{13}}{D(1-\mu)}\right\};\ \sigma_{23}=\frac{E}{1+\mu}\left\{\frac{Q_{23}}{K(1-\mu)}+\alpha_3\frac{R_{23}}{D(1-\mu)}\right\} \tag{2.73}$$

2.2.5 Equations of Equilibrium

The equations of equilibrium associated with the SSODM (Eqs. (2.61) – (2.63)) are also derived using the principle of virtual work.

The principle of virtual work yields for the present SSODM theory:

$$\begin{aligned}0&=\int_{\alpha_1}\int_{\alpha_2}\left[\int_{-h/2}^{h/2}\left(\sigma_{11}\delta\varepsilon_{11}+\sigma_{22}\delta\varepsilon_{22}+\sigma_{12}\delta\varepsilon_{12}+\sigma_{13}\delta\varepsilon_{13}+\sigma_{23}\delta\varepsilon_{23}\right)d\alpha_3-\left(q_1\delta u+q_2\delta v+q_3\delta w\right)\right]AB\,d\alpha_1 d\alpha_2\\&=\int_{\alpha_1}\int_{\alpha_2}\Big[N_{11}\delta\varepsilon_{11}^{(0)}+M_{11}\delta\kappa_{11}^{(0)}+L_{11}\delta\kappa_{11}^{(1)}+N_{22}\delta\varepsilon_{22}^{(0)}+M_{22}\delta\kappa_{22}^{(0)}+L_{22}\delta\kappa_{22}^{(1)}+N_{12}\delta\varepsilon_{12}^{(0)}+M_{12}\delta\kappa_{12}^{(0)}\\&\qquad+L_{12}\delta\kappa_{12}^{(1)}+Q_{13}\delta\varepsilon_{13}^{(0)}+R_{13}\delta\kappa_{13}^{(0)}+Q_{23}\delta\varepsilon_{23}^{(0)}+R_{23}\delta\kappa_{23}^{(0)}-q_1\delta u-q_2\delta v-q_3\delta w\Big]AB\,d\alpha_1 d\alpha_2\end{aligned} \tag{2.74}$$

By integrating by parts the displacement gradients associated with Eq. (2.74), the governing equations of static equilibrium are obtained from the resulting expressions by similarly setting the coefficients of variations δu, δv, δw, $\delta\varphi_1$, $\delta\varphi_2$, $\delta\psi_1$ and $\delta\psi_2$ to zero separately as:

$$\delta u:\frac{\partial(N_{11}B)}{\partial\alpha_1}-N_{22}\frac{\partial B}{\partial\alpha_1}+\frac{\partial(N_{21}A)}{\partial\alpha_2}+N_{12}\frac{\partial A}{\partial\alpha_2}+q_1AB=0 \tag{2.75}$$

$$\delta v:\frac{\partial(N_{22}A)}{\partial\alpha_2}-N_{11}\frac{\partial A}{\partial\alpha_2}+\frac{\partial(N_{12}B)}{\partial\alpha_1}+N_{21}\frac{\partial B}{\partial\alpha_1}+q_2AB=0 \tag{2.76}$$

$$\delta w: \frac{\partial(Q_{13}B)}{\partial\alpha_1}+\frac{\partial(Q_{23}A)}{\partial\alpha_2}-\left(\frac{N_{11}}{R_1}+\frac{N_{22}}{R_2}\right)+q_3AB=0 \tag{2.77}$$

$$\delta\varphi_1: \frac{\partial(M_{11}B)}{\partial\alpha_1}-M_{22}\frac{\partial B}{\partial\alpha_1}+\frac{\partial(M_{21}A)}{\partial\alpha_2}+M_{12}\frac{\partial A}{\partial\alpha_2}-Q_{13}AB=0 \tag{2.78}$$

$$\delta\varphi_2: \frac{\partial(M_{22}A)}{\partial\alpha_2}-M_{11}\frac{\partial A}{\partial\alpha_2}+\frac{\partial(M_{12}B)}{\partial\alpha_1}+M_{21}\frac{\partial B}{\partial\alpha_1}-Q_{23}AB=0 \tag{2.79}$$

$$\delta\psi_1: \frac{\partial(L_{11}B)}{\partial\alpha_1}-L_{22}\frac{\partial B}{\partial\alpha_1}+\frac{\partial(L_{21}A)}{\partial\alpha_2}+L_{12}\frac{\partial A}{\partial\alpha_2}-2R_{13}AB=0 \tag{2.80}$$

$$\delta\psi_2: \frac{\partial(L_{22}A)}{\partial\alpha_2}-L_{11}\frac{\partial A}{\partial\alpha_2}+\frac{\partial(L_{12}B)}{\partial\alpha_1}+L_{21}\frac{\partial B}{\partial\alpha_1}-2R_{23}AB=0 \tag{2.81}$$

2.2.6 Application of the Theory based on the SSODM to Circular Cylindrical Shells of Revolution

The differential equations of static equilibrium for the circular cylindrical shell based on the SSODM theory are now obtained by substituting Eqs. (2.39) and (2.40) into Eqs. (2.75) – (2.81) as:

$$\frac{\partial N_{xx}}{\partial x}+\frac{1}{a}\frac{\partial N_{\vartheta x}}{\partial\vartheta}+q_x=0 \tag{2.82}$$

$$\frac{\partial N_{x\vartheta}}{\partial x}+\frac{1}{a}\frac{\partial N_{\vartheta\vartheta}}{\partial\vartheta}+q_\vartheta=0 \tag{2.83}$$

$$\frac{\partial Q_{xz}}{\partial x}+\frac{1}{a}\frac{\partial Q_{\vartheta z}}{\partial\vartheta}-\frac{N_{\vartheta\vartheta}}{a}+q_z=0 \tag{2.84}$$

$$\frac{\partial M_{xx}}{\partial x}+\frac{1}{a}\frac{\partial M_{\vartheta x}}{\partial\vartheta}-Q_{xz}=0 \tag{2.85}$$

$$\frac{\partial M_{x\vartheta}}{\partial x}+\frac{1}{a}\frac{\partial M_{\vartheta\vartheta}}{\partial\vartheta}-Q_{\vartheta z}=0 \tag{2.86}$$

$$\frac{\partial L_{xx}}{\partial x}+\frac{1}{a}\frac{\partial L_{\vartheta x}}{\partial\vartheta}-2R_{xz}=0 \tag{2.87}$$

$$\frac{\partial L_{x\vartheta}}{\partial x}+\frac{1}{a}\frac{\partial L_{\vartheta\vartheta}}{\partial\vartheta}-2R_{\vartheta z}=0 \tag{2.88}$$

The equations of the strain components $\varepsilon_{xx}^{(0)},\kappa_{xx}^{(0)},\kappa_{xx}^{(1)},\varepsilon_{\vartheta\vartheta}^{(0)},\kappa_{\vartheta\vartheta}^{(0)},\kappa_{\vartheta\vartheta}^{(1)},\varepsilon_{x\vartheta}^{(0)},\kappa_{x\vartheta}^{(0)}$ and $\kappa_{x\vartheta}^{(1)}$ expressed in terms of displacements are also obtained as given in Eq. (2.48).

The transverse shear strain components expressed in terms of displacements for the circular cylindrical shell are now obtained with reference to Eq. (2.67) as:

$$\varepsilon_{xz}^{(0)}=\varphi_x+\frac{\partial w}{\partial x};\ \kappa_{xz}^{(0)}=2\psi_x;\ \varepsilon_{\vartheta z}^{(0)}=\varphi_\vartheta+\frac{1}{a}\frac{\partial w}{\partial\vartheta};\ \kappa_{\vartheta z}^{(0)}=2\psi_\vartheta \tag{2.89}$$

The expressions for the stress resultant – displacement relations for the stress resultants N_{xx}, $N_{\vartheta\vartheta}$, $N_{x\vartheta}$, M_{xx}, $M_{\vartheta\vartheta}$, $M_{x\vartheta}$, L_{xx}, $L_{\vartheta\vartheta}$ and $L_{x\vartheta}$ are also obtained as given in Eqs. (2.49) – (2.51).

The expressions for the stress resultant – displacement relations associated with the transverse shear are now obtained as:

$$Q_{xz}=\frac{K(1-\mu)}{2}\left[\frac{\partial w}{\partial x}+\varphi_x\right];\ Q_{\vartheta z}=\frac{K(1-\mu)}{2}\left[\frac{1}{a}\frac{\partial w}{\partial \vartheta}+\varphi_\vartheta\right];\ R_{xz}=D(1-\mu)\psi_x;\ R_{\vartheta z}=D(1-\mu)\psi_\vartheta \tag{2.90}$$

The equations of equilibrium (Eqs. (2.82) – (2.88)) are now expressed in terms of displacement components as:

$$\frac{\partial^2 u}{\partial x^2}+\left(\frac{1-\mu}{2a^2}\right)\frac{\partial^2 u}{\partial \vartheta^2}+\left(\frac{1+\mu}{2a}\right)\frac{\partial^2 v}{\partial \vartheta \partial x}+\frac{\mu}{a}\frac{\partial w}{\partial x}+\frac{h^2}{12}\frac{\partial^2 \psi_x}{\partial x^2}+\frac{h^2}{12}\left(\frac{1-\mu}{2a^2}\right)\frac{\partial^2 \psi_x}{\partial \vartheta^2}+\frac{h^2}{12}\left(\frac{1+\mu}{2a}\right)\frac{\partial^2 \psi_\vartheta}{\partial \vartheta \partial x}=-\frac{q_x(1-\mu^2)}{Eh} \tag{2.91}$$

$$\frac{\partial^2 u}{\partial x \partial \vartheta}\left(\frac{1+\mu}{2a}\right)+\left(\frac{1-\mu}{2}\right)\frac{\partial^2 v}{\partial x^2}+\frac{1}{a^2}\frac{\partial^2 v}{\partial \vartheta^2}+\frac{1}{a^2}\frac{\partial w}{\partial \vartheta}+\frac{h^2(1-\mu)}{24}\frac{\partial^2 \psi_\vartheta}{\partial x^2}+\frac{h^2}{12}\left(\frac{1+\mu}{2a}\right)\frac{\partial^2 \psi_x}{\partial x \partial \vartheta}+\frac{h^2}{12a^2}\frac{\partial^2 \psi_\vartheta}{\partial \vartheta^2}=-\frac{q_\vartheta(1-\mu^2)}{Eh} \tag{2.92}$$

$$\left(\frac{1-\mu}{2}\right)\frac{\partial^2 w}{\partial x^2}+\left(\frac{1-\mu}{2}\right)\frac{\partial \varphi_x}{\partial x}+\left(\frac{1-\mu}{2a^2}\right)\frac{\partial^2 w}{\partial \vartheta^2}+\left(\frac{1-\mu}{2a}\right)\frac{\partial \varphi_\vartheta}{\partial \vartheta}-\frac{1}{a^2}\frac{\partial v}{\partial \vartheta}-\frac{w}{a^2}-\frac{\mu}{a}\frac{\partial u}{\partial x}-\frac{h^2}{12}\frac{\mu}{a}\frac{\partial \psi_x}{\partial x}$$
$$-\frac{h^2}{12a^2}\frac{\partial \psi_\vartheta}{\partial \vartheta}=-\frac{q_z(1-\mu^2)}{Eh} \tag{2.93}$$

$$\frac{h^2}{12}\frac{\partial^2 \varphi_x}{\partial x^2}+\frac{h^2}{12}\left(\frac{1-\mu}{2a^2}\right)\frac{\partial^2 \varphi_x}{\partial \vartheta^2}-\frac{1-\mu}{2}\left(\varphi_x+\frac{\partial w}{\partial x}\right)+\frac{h^2}{12}\left(\frac{1+\mu}{2a}\right)\frac{\partial^2 \varphi_\vartheta}{\partial \vartheta \partial x}=0 \tag{2.94}$$

$$\frac{h^2(1-\mu)}{24}\left(\frac{\partial^2 \varphi_\vartheta}{\partial x^2}+\frac{\psi_\vartheta}{a}\right)+\frac{h^2}{12a^2}\frac{\partial^2 \varphi_\vartheta}{\partial \vartheta^2}-\frac{1-\mu}{2}\left(\varphi_\vartheta+\frac{\partial w}{\partial \vartheta}\frac{1}{a}\right)+\frac{h^2}{12}\left(\frac{1+\mu}{2a}\right)\frac{\partial^2 \varphi_x}{\partial \vartheta \partial x}=0 \tag{2.95}$$

$$\frac{h^2}{12}\left(\frac{\partial^2 u}{\partial x^2}+\frac{\mu}{a}\frac{\partial w}{\partial x}\right)+\frac{h^2}{80}\frac{\partial^2 \psi_x}{\partial x^2}+\frac{h^2}{12}\left(\frac{1-\mu}{2a^2}\right)\frac{\partial^2 u}{\partial \vartheta^2}+\frac{h^2(1-\mu)}{160a^2}\frac{\partial^2 \psi_x}{\partial \vartheta^2}-\frac{h^2(1-\mu)}{6}\psi_x+\frac{h^2}{12}\left(\frac{1+\mu}{2a}\right)\frac{\partial^2 v}{\partial \vartheta \partial x}$$
$$+\frac{h^2}{80}\left(\frac{1+\mu}{2a}\right)\frac{\partial^2 \psi_\vartheta}{\partial \vartheta \partial x}=0 \tag{2.96}$$

$$\frac{h^2}{12}\left(\frac{1+\mu}{2a}\right)\frac{\partial^2 u}{\partial x \partial \vartheta}+\frac{h^2(1-\mu)}{24}\frac{\partial^2 v}{\partial x^2}+\frac{h^2(1-\mu)}{160}\frac{\partial^2 \psi_\vartheta}{\partial x^2}+\frac{h^2}{80}\left(\frac{1+\mu}{2a}\right)\frac{\partial^2 \psi_x}{\partial x \partial \vartheta}+\frac{h^2}{12a^2}\frac{\partial w}{\partial \vartheta}-\frac{h^2(1-\mu)\psi_\vartheta}{6}$$
$$+\frac{h^2}{12a^2}\frac{\partial^2 v}{\partial \vartheta^2}+\frac{h^2}{80a^2}\frac{\partial^2 \psi_\vartheta}{\partial \vartheta^2}=0 \tag{2.97}$$

3 SOLUTION PROCEDURE

3.1 Boundary conditions

Here we consider a scenario where a circular cylindrical shell of finite length *l* is simply supported at its ends ($x = 0$, $x = l$) by shear diaphragms and subject to applied loading, the boundary conditions at both ends (Leissa, 1973; Nosier and Reddy, 1992; Di and Rothert, 1995) are of the form:

$$N_{xx} = M_{xx} = L_{xx} = \varphi_\vartheta = \psi_\vartheta = v = w = 0 \tag{3.1}$$

Nosier and Reddy (1992) referred to Eq. (3.1) as a simply supported boundary type S3 and further classified a combination of boundary conditions that can be assumed to exist at the edges of a shell for clamped, simply supported and free edges. The boundary condition Eq. (3.1) reasonably represent in physical application an attachment of a thin

perpendicular plate element possessing considerable stiffness in its plane to the boundary ends of the shell such that the ends are considerably stiffened to restrain the shell out-of-plane displacement component (w), in-plane tangential displacement component (v) and the generalized rotations (φ_ϑ , ψ_ϑ) about the x – axis. On account of the thinness of the attached plate element, very little stiffness is expected to be possessed in the x – axis transverse to its plane, thereby resulting in negligible axial moment resultants (M_{xx}, L_{xx}) and axial membrane force (N_{xx}) at the shell ends during deformation (Leissa, 1973).

3.2 Applied loading and method of solution

The solution of the equilibrium equations (Eqs. (2.54) – (2.60) and Eqs. (2.91) – (2.97)) for the FSODM and SSODM theories are obtained by use of the Navier solution approach. This approach requires that the applied load and displacement components be expanded in a double trigonometric Fourier series.

The applied load is assumed to be in the following form:

$$q_z = \sum_{m}^{\infty}\sum_{n}^{\infty} q_{mn} \cos n\vartheta \, Sin\frac{m\pi x}{l}; \quad q_x = q_\vartheta = 0 \tag{3.2}$$

where l is the length (span) of the cylindrical shell.

When the shell loading is uniformly distributed (UDL) the terms m, n are n = 0, 1 and m being a series of odd numbers (m = 1, 3, 5, 7, 9……), the coefficient q_{mn} of the Fourier trigonometric series (Eq. (3.2)) is given as $q_{m0} = q_{m1} = 4\gamma a/m\pi$ (Timoshenko and Woinowsky-Krieger, 1987; Ugural, 2010). However, for the case where the loading is of a sinusoidal nature (SDL) the coefficient is taken as $q_{mn} = q$ for m = 1 and n = 4, where q and γ represents the loading intensities and a represent the radius of the shell.

The Navier solutions of the displacement variables satisfying the equilibrium equations (Eqs. (2.54) – (2.60) and Eqs. (2.91) – (2.97)) and the force and essential boundary conditions (Eq. (3.1)) at the simply supported ends (x = 0, x = l) are introduced as:

$$u = \sum_{m=1}^{\infty}\sum_{n=0}^{\infty} A_{mn} Cos\frac{m\pi x}{l} Cos\, n\vartheta \; ; \; v = \sum_{m=1}^{\infty}\sum_{n=0}^{\infty} B_{mn} Sin\frac{m\pi x}{l} Sin\, n\vartheta \; ; \; w = \sum_{m=1}^{\infty}\sum_{n=0}^{\infty} C_{mn} Sin\frac{m\pi x}{l} Cos\, n\vartheta \; ;$$

$$\varphi_x = \sum_{m=1}^{\infty}\sum_{n=0}^{\infty} D_{mn} Cos\frac{m\pi x}{l} Cos\, n\vartheta \; ; \; \varphi_\vartheta = \sum_{m=1}^{\infty}\sum_{n=0}^{\infty} E_{mn} Sin\frac{m\pi x}{l} Sin\, n\vartheta \; ; \; \psi_x = \sum_{m=1}^{\infty}\sum_{n=0}^{\infty} F_{mn} Cos\frac{m\pi x}{l} Cos\, n\vartheta \; ;$$

$$\psi_\vartheta = \sum_{m=1}^{\infty}\sum_{n=0}^{\infty} G_{mn} Sin\frac{m\pi x}{l} Sin\, n\vartheta \tag{3.3}$$

where A_{mn}, B_{mn}, C_{mn}, D_{mn}, E_{mn}, F_{mn} and G_{mn} are undetermined coefficients.

Substituting Eqs. (3.2) and (3.3) into the equilibrium equations (Eqs. (2.54) – (2.60)) of the FSODM theory results in:

$$\begin{bmatrix} b_{11} & b_{12} & b_{13} & 0 & 0 & b_{16} & b_{17} \\ b_{21} & b_{22} & b_{23} & 0 & b_{25} & b_{26} & b_{27} \\ b_{31} & b_{32} & b_{33} & b_{34} & b_{35} & b_{36} & b_{37} \\ 0 & 0 & b_{43} & b_{44} & b_{45} & 0 & 0 \\ 0 & b_{52} & b_{53} & b_{54} & b_{55} & 0 & b_{57} \\ b_{61} & b_{62} & b_{63} & 0 & 0 & b_{66} & b_{67} \\ b_{71} & b_{72} & b_{73} & 0 & b_{75} & b_{76} & b_{77} \end{bmatrix} \begin{Bmatrix} A_{mn} \\ B_{mn} \\ C_{mn} \\ D_{mn} \\ E_{mn} \\ F_{mn} \\ G_{mn} \end{Bmatrix} = \begin{Bmatrix} 0 \\ 0 \\ -\dfrac{q_{mn}(1-\mu^2)}{Eh} \\ 0 \\ 0 \\ 0 \\ 0 \end{Bmatrix} \tag{3.4}$$

The coefficients of the matrix b_{ij} (i, j =1, 2,. . .5) are:

$$b_{11}=-\left[\left(\frac{m\pi}{l}\right)^2+\frac{n^2}{a^2}\left(\frac{1-\mu}{2}\right)\right];\ b_{12}=b_{21}=n\frac{m\pi}{l}\frac{1+\mu}{2a};\ b_{13}=b_{31}=\frac{\mu}{a}\frac{m\pi}{l};\ b_{16}=b_{61}=-\frac{h^2}{12}\left[\left(\frac{m\pi}{l}\right)^2+\frac{n^2}{a^2}\left(\frac{1-\mu}{2}\right)\right];$$

$$b_{17}=b_{71}=\frac{h^2}{12}\left(\frac{1+\mu}{2}\right)\frac{n}{a}\frac{m\pi}{l};\qquad b_{22}=-\left[\frac{1-\mu}{2}\left(\frac{m\pi}{l}\right)^2+\frac{n^2}{a^2}+\left(\frac{1-\mu}{2a^2}\right)\right];\qquad b_{23}=b_{32}=-\left(\frac{3-\mu}{2}\right)\frac{n}{a^2};\qquad b_{25}=b_{52}=\frac{1-\mu}{2a};$$

$$b_{26}=b_{62}=\frac{h^2}{12}\left(\frac{1+\mu}{2}\right)\frac{n}{a}\frac{m\pi}{l};\qquad b_{27}=b_{72}=-\frac{h^2}{12}\left[\frac{1-\mu}{2}\left(\frac{m\pi}{l}\right)^2+\frac{n^2}{a^2}+\left(\frac{1-\mu}{2a^2}\right)\right];\qquad b_{33}=-\left[\frac{1-\mu}{2}\left(\frac{m\pi}{l}\right)^2+\frac{1}{a^2}+\left(\frac{1-\mu}{2a^2}\right)n^2\right];$$

$$b_{34}=b_{43}=-\left(\frac{1-\mu}{2}\right)\frac{m\pi}{l};\qquad b_{35}=b_{53}=\left(\frac{1-\mu}{2a}\right)n;\qquad b_{36}=b_{63}=\frac{h^2}{12}\frac{\mu}{a}\frac{m\pi}{l};\qquad b_{37}=b_{73}=-\frac{h^2}{12}\left(\frac{3-\mu}{2}\right)\frac{n}{a^2};$$

$$b_{44}=-\frac{(1-\mu)}{2}-\frac{h^2}{12}\left(\frac{m\pi}{l}\right)^2-\frac{h^2(1-\mu)}{24}\frac{n^2}{a^2};\qquad b_{45}=b_{54}=\frac{h^2}{12}\left(\frac{1+\mu}{2}\right)\frac{n}{a}\frac{m\pi}{l};\qquad b_{55}=-\frac{(1-\mu)}{2}-\frac{h^2}{12}\frac{n^2}{a^2}-\frac{h^2(1-\mu)}{24}\left(\frac{m\pi}{l}\right)^2;$$

$$b_{57}=b_{75}=\frac{h^2(1-\mu)}{24a};\qquad b_{66}=-\frac{h^2}{80}\left[\left(\frac{m\pi}{l}\right)^2+\frac{n^2}{a^2}\left(\frac{1-\mu}{2}\right)+\frac{40}{3}(1-\mu)\right];\qquad b_{67}=b_{76}=\frac{h^2}{80}\left(\frac{1+\mu}{2}\right)\frac{n}{a}\frac{m\pi}{l};$$

$$b_{77}=-\frac{h^2}{80}\left[\frac{1-\mu}{2}\left(\frac{m\pi}{l}\right)^2+\frac{n^2}{a^2}+\frac{40}{3}(1-\mu)+\left(\frac{1-\mu}{2a^2}\right)\right] \tag{3.5}$$

Also, substituting Eqs. (3.2) and (3.3) into the equilibrium equations (Eqs. (2.91) – (2.97)) of the SSODM theory results in:

$$\begin{bmatrix} d_{11} & d_{12} & d_{13} & 0 & 0 & d_{16} & d_{17} \\ d_{21} & d_{22} & d_{23} & 0 & 0 & d_{26} & d_{27} \\ d_{31} & d_{32} & d_{33} & d_{34} & d_{35} & d_{36} & d_{37} \\ 0 & 0 & d_{43} & d_{44} & d_{45} & 0 & 0 \\ 0 & 0 & d_{53} & d_{54} & d_{55} & 0 & 0 \\ d_{61} & d_{62} & d_{63} & 0 & 0 & d_{66} & d_{67} \\ d_{71} & d_{72} & d_{73} & 0 & 0 & d_{76} & d_{77} \end{bmatrix}\begin{Bmatrix} A_{mn} \\ B_{mn} \\ C_{mn} \\ D_{mn} \\ E_{mn} \\ F_{mn} \\ G_{mn} \end{Bmatrix}=\begin{Bmatrix} 0 \\ 0 \\ -\dfrac{q_{mn}(1-\mu^2)}{Eh} \\ 0 \\ 0 \\ 0 \\ 0 \end{Bmatrix} \tag{3.6}$$

The coefficients of the matrix d_{ij} (i, j =1, 2,. . .5) are:

$$d_{11}=-\left[\left(\frac{m\pi}{l}\right)^2+\frac{n^2}{a^2}\left(\frac{1-\mu}{2}\right)\right];\qquad d_{12}=d_{21}=n\frac{m\pi}{l}\frac{1+\mu}{2a};\qquad d_{13}=d_{31}=\frac{\mu}{a}\frac{m\pi}{l};\qquad d_{16}=d_{61}=-\frac{h^2}{12}\left[\left(\frac{m\pi}{l}\right)^2+\frac{n^2}{a^2}\left(\frac{1-\mu}{2}\right)\right];$$

$$d_{17}=d_{71}=\frac{h^2}{12}\left(\frac{1+\mu}{2}\right)\frac{n}{a}\frac{m\pi}{l};\qquad d_{22}=-\left[\frac{1-\mu}{2}\left(\frac{m\pi}{l}\right)^2+\frac{n^2}{a^2}\right];\qquad d_{23}=d_{32}=-\frac{n}{a^2};\qquad d_{26}=d_{62}=\frac{h^2}{12}\left(\frac{1+\mu}{2}\right)\frac{n}{a}\frac{m\pi}{l};$$

$$d_{27}=d_{72}=-\frac{h^2}{12}\left[\frac{1-\mu}{2}\left(\frac{m\pi}{l}\right)^2+\frac{n^2}{a^2}\right];\qquad d_{33}=-\left[\frac{1-\mu}{2}\left(\frac{m\pi}{l}\right)^2+\frac{1}{a^2}+\left(\frac{1-\mu}{2a^2}\right)n^2\right];\qquad d_{34}=d_{43}=-\left(\frac{1-\mu}{2}\right)\frac{m\pi}{l};$$

$$d_{35}=d_{53}=\left(\frac{1-\mu}{2a}\right)n;\ d_{36}=d_{63}=\frac{h^2}{12}\frac{\mu}{a}\frac{m\pi}{l};\qquad d_{37}=d_{73}=-\frac{h^2}{12}\frac{n}{a^2};\qquad d_{44}=-\frac{(1-\mu)}{2}-\frac{h^2}{12}\left(\frac{m\pi}{l}\right)^2-\frac{h^2(1-\mu)}{24}\frac{n^2}{a^2};$$

$$d_{45}=d_{54}=\frac{h^2}{12}\left(\frac{1+\mu}{2}\right)\frac{n}{a}\frac{m\pi}{l};\quad d_{55}=-\frac{(1-\mu)}{2}-\frac{h^2}{12}\frac{n^2}{a^2}-\frac{h^2(1-\mu)}{24}\left(\frac{m\pi}{l}\right)^2;\quad d_{66}=-\frac{h^2}{80}\left[\left(\frac{m\pi}{l}\right)^2+\frac{n^2}{a^2}\left(\frac{1-\mu}{2}\right)+\frac{40}{3}(1-\mu)\right];$$

$$d_{67}=d_{76}=\frac{h^2}{80}\left(\frac{1+\mu}{2}\right)\frac{n}{a}\frac{m\pi}{l};\ d_{77}=-\frac{h^2}{80}\left[\frac{1-\mu}{2}\left(\frac{m\pi}{l}\right)^2+\frac{n^2}{a^2}+\frac{40}{3}(1-\mu)\right] \tag{3.7}$$

From the coefficients of the resulting displacement matrices (Eqs. (3.5) and (3.7)), one can easily observe that the displacement components in the derived equations of static equilibrium (Eqs. (2.54) – (2.60) and Eqs. (2.91) – (2.97)) associated with both developed second-order shear deformation theories are symmetric on account of symmetry of the shear stresses. By solving the complete matrices for the undetermined parameters A_{mn}, B_{mn}, C_{mn}, D_{mn}, E_{mn}, F_{mn} and G_{mn}, the numerical values of the displacements and stresses can then be computed.

4 RESULTS AND DISCUSSION

In this section, the developed second-order shear deformation theories (FSODM and SSODM theories) are employed in solving problems associated with the static bending response of circular cylindrical shells under simply supported boundary conditions. The numerical results of the displacements and stresses are presented in tables. Comparisons are made to results of the classical shell theory – CST (Soedel, 2004), first-order shear deformation theory – FSDT (Khdeir et al., 1989) and higher-order shear deformation theory – HSDT (Nwoji et al., 2021) in order to ascertain their suitability in usage.

The illustrative examples considered by Nwoji et al. (2021) are adopted here.

Example one: The maximum deflection, axial and circumferential stresses for a simply (diaphragms) supported circular cylindrical shell of elastic modulus E filled with liquid (UDL) of specific weight γ are to be obtained for the following parameters: a = 50cm; l = 25cm; μ = 0.3, while using the first three terms of the series m i.e., m = 1, 3, 5 at chosen values of radius to thickness ratios $S = a/h$.

The results are presented in the following non-dimensional definitions (Nwoji et al., 2021)

$$\overline{w}=\left(\frac{10Eh^3}{\gamma a^4}\right)w;\ \overline{\sigma}_x=\left(\frac{10h^2}{\gamma a^2}\right)\sigma_x;\ \overline{\sigma}_\vartheta=\left(\frac{10h^2}{\gamma a^2}\right)\sigma_\vartheta \tag{4.1}$$

The maximum values of the displacements, forces and moments are obtained at the mid-span ($x = l/2$; $\vartheta = 0$)

Example two: The problem of obtaining the displacements and stresses for the simply (diaphragms) supported shell now subject to sinusoidal transverse surface load (SDL) for chosen values of S at varying length to radius ratios l/a is considered using the following parameters: a = 50cm; l = 25cm, 125cm, 250cm and 500cm; μ = 0.3.

The results are presented in the following non – dimensional definitions (Di and Rothert, 1995).

$$(\overline{w},\overline{v},\overline{\sigma}_\vartheta,\overline{\sigma}_x)=\left[\left(\frac{10Eh^3}{qa^4}\right)w,\left(\frac{10Eh^2}{qa^3}\right)v,\left(\frac{10h^2}{qa^2}\right)\sigma_\vartheta,\left(\frac{10h^2}{qa^2}\right)\sigma_x\right]\Big/\cos n\vartheta\sin\frac{m\pi x}{l};\ \overline{\sigma}_{x\vartheta}=\left(\frac{10h^2}{qa^2}\right)\sigma_{x\vartheta}\Big/\sin n\vartheta\cos\frac{m\pi x}{l};$$

$$(\overline{u},\overline{\sigma}_{xz})=\left[\left(\frac{10Eh^2}{qa^3}\right)u,\left(\frac{10h}{qa}\right)\sigma_{xz}\right]\Big/\cos n\vartheta\cos\frac{m\pi x}{l};\ \overline{\sigma}_{\vartheta z}=\left(\frac{10h}{qa}\right)\sigma_{\vartheta z}\Big/\sin n\vartheta\sin\frac{m\pi x}{l} \tag{4.2}$$

The obtained results from both second-order shear deformation shell theories are presented in Tables 1 – 7. Comparisons are made to those obtained by the Love – Kirchhoff classical shell theory – CST (Soedel, 2004), first-order shear deformation theory – FSDT (Khdeir et al., 1989) and higher-order shear deformation theory – HSDT (Nwoji et al., 2021) for chosen radius to thickness ratios ($S = a/h$) at varying length to radius of curvature ratios (l/a). A close examination of the non-dimensional deflection as presented in Table 1 for the cylindrical shell under uniformly distributed loading (UDL) at l/a = 0.5 reveals that the results of the shell theories formulated on the FSODM and SSODM are in close agreement with those of the CST; FSDT; HSDT for the thin shell cases (S =

100, 20) and FSDT; HSDT for the moderately thick case (S = 10). While for the very thick case (S = 4), the results of both second-order theories are close to those of the HSDT although lower within 6% variations.

Table 2 presents the convergence study for the non-dimensional deflection and stresses for the shell under UDL at l/a = 0.5. The results show that the trigonometric series Eq. (3.3) converges faster for deflections than stresses, the convergence in deflections are found to be slower in thick shells than thin shells. Furthermore, one realizes that the adoption of only the first three terms of the series m as recommended by Timoshenko and Woinowsky-Krieger (1987) obtains the deformation of the shell with sufficient accuracy for its thin and thick cases (S = 20, 10, 4) and the error of solution due to the finite summation are obtained within 0.1% for the deflections and 1% for the stresses. However, this is not the scenario for the very thin shell case (S = 100) where the error of solution for deflections are obtained within 0.5%; circumferential stresses within 1.5% and the axial stresses within 725%, thus requiring a considerable number of terms in order to achieve convergence as presented in Table 2. Generally, for all shell cases (S = 100, 20, 10, 4) the error in solution for the deflections introduced by adopting the first three terms in the series m are all within 0.5%.

For the case of the sinusoidal distributed loading (SDL) as presented in Tables 3, 4, 5 and 6 for l/a = 0.5, 2.5, 5 and 10 respectively. The results of the non-dimensional displacements for l/a = 0.5 obtained by the present FSODM and SSODM theories; just as in the case of the UDL are also in close agreement with those of the CST; FSDT; HSDT for the thin cases and FSDT; HSDT for the moderately thick cases. The results equally shows that the theory formulated on the first second-order displacement Model (FSODM) predicts noticeable higher values of the displacements when compared to those of the theory formulated on the second second-order displacement Model (SSODM), FSDT and HSDT. It was also observed that the variations in results recorded by the FSODM theory tend to magnify with increasing l/a ratios, with the greater effect of this magnification observed in the thin shell cases (S = 100, 20) when compared to the CST; FSDT; HSDT. The variations in displacements for the thin cases (S = 100, 20) as obtained by the FSODM theory are within 13%, 14.8% and 15% for l/a ratios = 2.5, 5 and 10 respectively.

Table 1 Non-dimensional results of the maximum deflection ($\overline{w}$), axial ($\overline{\sigma}_x$) and circumferential ($\overline{\sigma}_\vartheta$) stresses for simply supported (SS) circular cylindrical tank filled to capacity (UDL) for l/a = 0.5

S	Models		$\overline{w}$	$\overline{\sigma}_x$	$\overline{\sigma}_\vartheta$
100	**CST** (Soedel, 2004)		0.1115	0.5070	109.720
	FSDT (Khdeir et al., 1989)		0.1119	0.4330	109.880
	Present study	**-1**	0.1119	0.4324	109.909
		-2	0.1119	0.4331	109.929
	HSDT (Nwoji et al., 2021)		0.1115	0.5163	109.713
20	**CST** (Soedel, 2004)		23.404	468.953	601.293
	FSDT (Khdeir et al., 1989)		23.643	463.841	604.305
	Present study	**-1**	23.652	463.990	604.263
		-2	23.643	463.845	604.515
	HSDT (Nwoji et al., 2021)		23.519	459.798	600.660
10	**CST** (Soedel, 2004)		51.860	1.087.640	843.300
	FSDT (Khdeir et al., 1989)		54.661	1.050.720	858.950
	Present study	**-1**	54.707	1.051.649	858.580
		-2	54.661	1.050.730	859.194
	HSDT (Nwoji et al., 2021)		54.997	1.053.820	863.211
4	**CST**(Soedel, 2004)		78.292	1.660.212	821.814
	FSDT (Khdeir et al., 1989)		116.806	1.571.320	943.763
	Present study	**-1**	116.953	1.574.040	941.761
		-2	116.806	1.571.333	943.976
	HSDT (Nwoji et al., 2021)		123.634	1.708.750	1.013.390

Note: The results of the present study denoted as **(1)** and **(2)** represent those obtained by the FSODM and SSODM theories respectively

Table 2 Convergence study for non-dimensional deflection, axial and circumferential stresses for simply supported (SS) circular cylindrical shell under UDL for l/a = 0.5

N	*S* = 100			*S* = 20			*S* = 10			*S* = 4		
	$\overline{w}$	$\overline{\sigma}_x$	$\overline{\sigma}_\vartheta$	$\overline{w}$	$\overline{\sigma}_x$	$\overline{\sigma}_\vartheta$	$\overline{w}$	$\overline{\sigma}_x$	$\overline{\sigma}_\vartheta$	$\overline{w}$	$\overline{\sigma}_x$	$\overline{\sigma}_\vartheta$
3	0.1119	0.4324	10.9909	2.3652	46.3990	60.4263	5.4707	105.1649	85.8580	11.6953	157.4040	94.1761
6	0.1115	-0.0023	10.8160	2.3643	45.9560	60.2750	5.4684	104.7219	85.7015	11.6828	156.9610	93.9934
9	0.1115	0.0685	10.8412	2.3644	46.0261	60.2979	5.4687	104.7941	85.7264	11.6847	157.0320	94.0222
12	0.1115	0.0458	10.8340	2.3643	46.0034	60.29067	5.4686	104.7713	85.7185	11.6841	157.0080	94.0127
15	0.1115	0.0563	10.8372	2.3643	46.0138	60.2939	5.4687	104.7819	85.7221	11.6844	157.0190	94.0170
18	0.1115	0.0506	10.8355	2.3643	46.0082	60.2921	5.4686	104.7764	85.7202	11.6842	157.0130	94.0147
21	0.1115	0.0540	10.8365	2.3643	46.0116	60.2932	5.4686	104.7798	85.7214	11.6843	157.0170	94.0161
24	0.1115	0.0518	10.8359	2.3643	46.0094	60.2925	5.4686	104.7776	85.7206	11.6843	157.0150	94.0152
27	0.1115	0.0533	10.8363	2.3643	46.0109	60.2930	5.4686	104.7791	85.7211	11.6843	157.0160	94.0158
30	0.1115	0.0523	10.8360	2.3643	46.0098	60.2926	5.4686	104.7780	85.7208	11.6843	157.0150	94.0153
33	0.1115	0.0530	10.8362	2.3643	46.0106	60.2929	5.4686	104.7788	85.7211	11.6843	157.0160	94.0157
36	0.1115	0.0524	10.8361	2.3643	46.0101	60.2927	5.4686	104.7782	85.7209	11.6843	157.0150	94.0154
39	0.1115	0.0529	10.8362	2.3643	46.0105	60.2929	5.4686	104.7787	85.7210	11.6843	157.0160	94.0156
42	0.1115	0.0525	10.8361	2.3643	46.0101	60.2927	5.4686	104.7783	85.7209	11.6843	157.0150	94.0155
45	0.1115	0.0528	10.8362	2.3643	46.0105	60.2928	5.4686	104.7786	85.7210	11.6843	157.0160	94.0156
48	0.1115	0.0526	10.8361	2.3643	46.0101	60.2928	5.4686	104.7784	85.7209	11.6843	157.0150	94.0155
51	0.1115	0.0528	10.8362	2.3643	46.0104	60.2928	5.4686	104.7786	85.7210	11.6843	157.0160	94.0156
54	0.1115	0.0526	10.8361	2.3643	46.0102	60.2928	5.4686	104.7784	85.7209	11.6843	157.0150	94.0155
57	0.1115	0.0527	10.8362	2.3643	46.0104	60.2928	5.4686	107.7785	85.7210	11.6843	157.0156	94.0156
60	0.1115	0.0526	10.8361	2.3643	46.0103	60.2928	5.4686	107.7784	85.7210	11.6843	157.0155	94.0155
63	0.1115	0.0527	10.8361	2.3643	46.0104	60.2928	5.4686	107.7785	85.7210	11.6843	157.0156	94.0156
66	0.1115	0.0526	10.8361	2.3643	46.0103	60.2928	5.4686	107.7784	85.7210	11.6843	157.0154	94.0155
69	0.1115	0.0526	10.8361	2.3643	46.0103	60.2928	5.4686	107.7784	85.7210	11.6843	157.0155	94.0155
72	0.1115	0.0526	10.8361	2.3643	46.0103	60.2928	5.4686	107.7784	85.7210	11.6843	157.0155	94.0155
75	0.1115	0.0526	10.8361	2.3643	46.0103	60.2928	5.4686	107.7784	85.7210	11.6843	157.0155	94.0155
N	*S* = 100			*S* = 20			*S* = 10			*S* = 4		
	$\overline{w}$	$\overline{\sigma}_x$	$\overline{\sigma}_\vartheta$	$\overline{w}$	$\overline{\sigma}_x$	$\overline{\sigma}_\vartheta$	$\overline{w}$	$\overline{\sigma}_x$	$\overline{\sigma}_\vartheta$	$\overline{w}$	$\overline{\sigma}_x$	$\overline{\sigma}_\vartheta$
3	0.1119	0.4331	10.9929	2.3643	46.3845	60.4515	5.4661	105.0730	85.9194	11.6806	157.1333	94.3976
6	0.1115	-0.0016	10.8180	2.3633	45.9415	60.3002	5.4638	104.6300	85.7628	11.6681	156.6905	94.2150
9	0.1115	0.0686	10.8412	2.3634	46.0116	60.3232	5.4641	104.7020	85.7877	11.6701	156.7608	94.2437
12	0.1115	0.0458	10.8340	2.3634	45.9889	60.3158	5.4640	104.6790	85.7798	11.6694	156.7375	94.2342
15	0.1115	0.0563	10.8372	2.3634	45.9994	60.3191	5.4640	104.6900	85.7835	11.6697	156.7481	94.2385
18	0.1115	0.0506	10.8355	2.3634	45.9937	60.3173	5.4640	104.6840	85.7816	11.6696	156.7425	94.2362
21	0.1115	0.0540	10.8365	2.3634	45.9971	60.3184	5.4640	104.6860	85.7827	11.6697	156.7459	94.2376
24	0.1115	0.0518	10.8359	2.3634	45.9949	60.3177	5.4640	104.6870	85.7820	11.6696	156.7437	94.2367
27	0.1115	0.0533	10.8363	2.3634	45.9964	60.3182	5.4640	104.6860	85.7825	11.6696	156.7452	94.2373
30	0.1115	0.0523	10.8360	2.3634	45.9953	60.3179	5.4640	104.6870	85.7821	11.6696	156.7441	94.2369
33	0.1115	0.0530	10.8362	2.3634	45.9961	60.3181	5.4640	104.6860	85.7824	11.6696	156.7449	94.2372
36	0.1115	0.0524	10.8361	2.3634	45.9955	60.3179	5.4640	104.6870	85.7822	11.6696	156.7443	94.2370
39	0.1115	0.0529	10.8362	2.3634	45.9960	60.3181	5.4640	104.6860	85.7824	11.6696	156.7448	94.2371
42	0.1115	0.0525	10.8361	2.3634	45.9956	60.3180	5.4640	104.6870	85.7822	11.6696	156.7444	94.2370
45	0.1115	0.0528	10.8362	2.3634	45.9959	60.3180	5.4640	104.6860	85.7823	11.6696	156.7447	94.2371
48	0.1115	0.0526	10.8361	2.3634	45.9957	60.3180	5.4640	104.6860	85.7823	11.6696	156.7445	94.2370
51	0.1115	0.0528	10.8362	2.3634	45.9959	60.3180	5.4640	104.6860	85.7823	11.6696	156.7447	94.2371
54	0.1115	0.0526	10.8361	2.3634	45.9957	60.3180	5.4640	104.6860	85.7823	11.6696	156.7445	94.2370
57	0.1115	0.0527	10.8362	2.3634	45.9959	60.3180	5.4640	104.6860	85.7823	11.6696	156.7447	94.2371
60	0.1115	0.0526	10.8361	2.3634	45.9958	60.3180	5.4640	104.6860	85.7823	11.6696	156.7445	94.2371
63	0.1115	0.0526	10.8361	2.3634	45.9959	60.3180	5.4640	104.6860	85.7823	11.6696	156.7446	94.2371
66	0.1115	0.0526	10.8361	2.3634	45.9958	60.3180	5.4640	104.6860	85.7823	11.6696	156.7446	94.2371
69	0.1115	0.0526	10.8361	2.3634	45.9958	60.3180	5.4640	104.6860	85.7823	11.6696	156.7446	94.2371
72	0.1115	0.0526	10.8361	2.3634	45.9958	60.3180	5.4640	104.6860	85.7823	11.6696	156.7446	94.2371
75	0.1115	0.0526	10.8361	2.3634	45.9958	60.3180	5.4640	104.6860	85.7823	11.6696	156.7446	94.2371

Note: *N* represents the number of adopted terms in the series *m*

Table 3 Non-dimensional deflection $\overline{w}$, in-plane displacements $\overline{u}$, $\overline{v}$; in-plane normal stresses $\overline{\sigma}_x$, $\overline{\sigma}_\vartheta$; in-plane shear stress $\overline{\sigma}_{x\vartheta}$ for simply supported (SS) circular cylindrical shell under sinusoidal loading (SDL) for *l/a* = 0.5

S	Models		$\overline{w}$	$\overline{u}$	$\overline{v}$	$\overline{\sigma}_x\left(\alpha_3=\pm h/2\right)$	$\overline{\sigma}_\vartheta\left(\alpha_3=\pm h/2\right)$	$\overline{\sigma}_{x\vartheta}\left(\alpha_3=\pm h/2\right)$
100	**CST** (Soedel, 2004)		0.0019	-0.0016	-0.0260	0.0839	0.1234	-0.0422
						-0.0071	0.0661	-0.0784
	FSDT (Khdeir et al., 1989)		0.0019	-0.0016	-0.0264	0.0852	0.1253	-0.0429
						-0.0072	0.0672	-0.0796
	Present Study	**(1)**	0.0019	-0.0016	-0.0264	0.0852	0.1248	-0.0433
						-0.0070	0.0678	-0.0794
		(2)	0.0019	-0.0016	-0.0264	0.0852	0.1253	-0.0429
						-0.0072	0.0672	-0.0797
	HSDT (Nwoji et al., 2021)		0.0019	-0.0016	-0.0260	0.0838	0.1233	-0.0423
						-0.0070	0.0662	-0.0784
20	**CST** (Soedel, 2004)		0.0206	-0.0035	-0.0573	0.5872	0.5250	0.0665
						-0.4176	-0.1068	-0.3327
	FSDT (Khdeir et al., 1989)		0.0212	-0.0036	-0.0587	0.5860	0.5283	0.0617
						-0.4122	-0.0993	-0.3349
	Present Study	**(1)**	0.0214	-0.0039	-0.0603	0.5920	0.5252	0.0573
						-0.4141	-0.0967	-0.3367
		(2)	0.0212	-0.0036	-0.0588	0.5860	0.5284	0.0616
						-0.4121	-0.0992	-0.3349
	HSDT (Nwoji et al., 2021)		0.0211	-0.0036	-0.0586	0.5836	0.5263	0.0613
						-0.4103	-0.0987	-0.3336
10	**CST** (Soedel, 2004)		0.0301	-0.0026	-0.0418	0.7937	0.6126	0.1939
						-0.6702	-0.3080	-0.3878
	FSDT (Khdeir et al., 1989)		0.0334	-0.0028	-0.0462	0.7882	0.6218	0.1780
						-0.6509	-0.2830	-0.3937
	Present Study	**(1)**	0.0340	-0.0037	-0.0495	0.8019	0.6142	0.1713
						-0.6567	-0.2860	-0.3993
		(2)	0.0335	-0.0028	-0.0464	0.7882	0.6219	0.1779
						-0.6508	-0.2829	-0.3937
	HSDT (Nwoji et al., 2021)		0.0340	-0.0029	-0.0472	0.8026	0.6331	0.1815
						-0.6630	-0.2886	-0.4008
4	**CST** (Soedel, 2004)		0.0345	-0.0012	-0.0192	0.8677	0.5977	0.2890
						-0.8110	-0.4579	-0.3780
	FSDT (Khdeir et al., 1989)		0.0616	-0.0020	-0.0343	0.8714	0.6410	0.2468
						-0.7704	-0.3916	-0.4056
	Present Study	**(1)**	0.0629	-0.0045	-0.0414	0.8962	0.6158	0.2318
						-0.7776	-0.4083	-0.4183
		(2)	0.0616	-0.0021	-0.0342	0.8714	0.6411	0.2468
						-0.7703	-0.3915	-0.4056
	HSDT (Nwoji et al., 2021)		0.0664	-0.0023	-0.0369	1.0038	0.7318	0.2916
						-0.8947	-0.4625	-0.4629

These results recorded by the FSODM theory for the thin shell cases nevertheless constitutes a discrepancy which is in contradiction to the Known Love – Kirchhoff kinematic postulation of negligible transverse shear effect on the deformation of thin isotropic shells. A fact which is consistent with the findings of Soldatos (1986), Reddy (2007), Nwoji et al. (2021) and numerous other literatures on thick structural shells. It can equally be observed that this magnification in variations through increasing *l/a* ratios experienced by the FSODM theory is not present in the SSODM theory which variations in obtained results are within 5%, 3% and 1% for *l/a* ratios = 2.5, 5 and 10 respectively. The results of the displacements obtained by SSODM theory are found to be in good agreement with those of the CST; FSDT; HSDT for the thin shell cases (*S* = 100, 20) regardless of the *l/a* ratios considered.

The variations in numerical results between the shell theories recorded in percentages are defined as follows:

$$\%\,Difference = \frac{present\ theory - other\ theory}{other\ theory}\ x\ 100$$

A look at the results of the stresses for the UDL and SDL load cases presented in Tables 1 and 3 for *l/a* = 0.5 shows that the FSODM and SSODM theories predicts close enough results to those predicted by the CST; FSDT; HSDT for the thin shell cases (*S* = 100, 20). Table 1 reveals that for the case of the UDL, the in-plane axial stresses predicted by both

theories are significantly lower within 15% for the very thin case (*S* = 100) when compared to the HSDT. The results are in good agreement for the moderately thick case (*S* = 10), although are lower than those of the HSDT for the very thick case (*S* = 4). For higher ratios of *l/a* as presented in Tables 4, 5 and 6, the results presented by the SSODM theory for the SDL load case appear to be in more of an agreement with those of the CST (thin shell cases only); FSDT; HSDT than the results of the FSODM theory for the thin and moderately thick shell cases.

Table 4 Non-dimensional deflection $\overline{w}$, in-plane displacements $\overline{u}$, $\overline{v}$; in-plane normal stresses $\overline{\sigma}_x$, $\overline{\sigma}_\vartheta$; in-plane shear stress $\overline{\sigma}_{x\vartheta}$ for simply supported (SS) circular cylindrical shell under sinusoidal loading (SDL) for *l/a* = 2.5

S	Models		$\overline{w}$	$\overline{u}$	$\overline{v}$	$\overline{\sigma}_x\left(\alpha_3=\pm h/2\right)$	$\overline{\sigma}_\vartheta\left(\alpha_3=\pm h/2\right)$	$\overline{\sigma}_{x\vartheta}\left(\alpha_3=\pm h/2\right)$
100	**CST** (Soedel, 2004)		0.0917	-0.5786	-2.3292	1.0708	0.9040	-0.0584
						0.4280	-0.7558	-0.4129
	FSDT (Khdeir et al., 1989)		0.0946	-0.5974	-2.4046	1.1056	0.9332	-0.0603
						0.4422	-0.7797	-0.4263
	Present Study	**(1)**	0.0976	-0.6160	-2.4794	1.1235	0.9061	-0.0681
						0.4723	-0.7508	-0.4334
		(2)	0.0946	-0.5974	-2.4046	1.1058	0.9332	-0.0603
						0.4425	-0.7797	-0.4262
	HSDT (Nwoji et al., 2021)		0.0903	-0.5701	-2.2946	1.0545	0.8893	-0.0576
						0.4223	-0.7435	-0.4063
20	**CST** (Soedel, 2004)		0.3172	-0.4004	-1.6118	1.6305	2.9227	0.4503
						-0.5933	-2.8202	-0.7764
	FSDT (Khdeir et al., 1989)		0.3215	-0.4058	-1.6342	1.6416	2.9328	0.4502
						-0.5901	-2.8296	-0.7810
	Present Study	**(1)**	0.3577	-0.4546	-1.8246	1.7626	3.0372	0.4805
						-0.6011	-2.9764	-0.8456
		(2)	0.3215	-0.4060	-1.6342	1.6417	2.9328	0.4501
						-0.5899	-2.8296	-0.7808
	HSDT (Nwoji et al., 2021)		0.3200	-0.4041	-1.6266	1.6327	2.9165	0.4474
						-0.5859	-2.8131	-0.7763
10	**CST** (Soedel, 2004)		0.3436	-0.2169	-0.8730	1.4854	3.1384	0.5761
						-0.9236	-3.0828	-0.7527
	FSDT (Khdeir et al., 1989)		0.3579	-0.2260	-0.9095	1.4975	3.1397	0.5726
						-0.9121	-3.0821	-0.7567
	Present Study	**(1)**	0.4021	-0.2603	-1.0359	1.6073	3.2488	0.6227
						-0.9689	-3.3025	-0.8234
		(2)	0.3580	-0.2260	-0.9097	1.4975	3.1396	0.5725
						-0.9120	-3.0821	-0.7566
	HSDT (Nwoji et al., 2021)		0.3601	-0.2274	-0.9151	1.5057	3.1563	0.5754
						-0.9165	-3.0982	-0.7604
4	**CST** (Soedel, 2004)		0.3518	-0.0888	-0.3576	1.3483	3.1963	0.6441
						-1.1183	-3.1738	-0.7164
	FSDT (Khdeir et al., 1989)		0.4434	-0.1120	-0.4509	1.3773	3.1964	0.6342
						-1.0873	-3.1677	-0.7254
	Present Study	**(1)**	0.5012	-0.1430	-0.5456	1.4630	3.2211	0.7019
						-1.1850	-3.4929	-0.7893
		(2)	0.4424	-0.1120	-0.4507	1.3777	3.1974	0.6343
						-1.0874	-3.1686	-0.7253
	HSDT (Nwoji et al., 2021)		0.4611	-0.1165	-0.4686	1.4396	3.3391	0.6644
						-1.1379	-3.3091	-0.7592

The variations in results between those predicted by the FSODM theory and those of the HSDT; FSDT; CST for the in-plane normal and shear stresses under SDL for the thin cases (*S* = 100, 20) are within 3%, 16%, 30% and 11% for *l/a* ratios = 0.5, 2.5, 5 and 10 respectively, while those of the SSODM theory are within 2%, 4%, 3% and 1% for *l/a* ratios = 0.5, 2.5, 5 and 10 respectively. The results show that increment in ratios of *l/a* = 2.5 – 10 leads to substantial errors in results of the displacements and stresses obtained by the FSODM theory for the thin shell cases. The results equally highlights the inability of the FSODM theory to predict acceptable values of the displacements and stresses within the admissible engineering error (5%) when applied to thin shells at high *l/a* ratios. Generally, the accuracy of the FSODM theory has been found to significantly diminish with continual increase in *l/a* ratios.

Table 5 Non-dimensional deflection $\overline{w}$, in-plane displacements $\overline{u}$, $\overline{v}$; in-plane normal stresses $\overline{\sigma}_x$, $\overline{\sigma}_\vartheta$; in-plane shear stress $\overline{\sigma}_{x\vartheta}$ for simply supported (SS) circular cylindrical shell under sinusoidal loading (SDL) for *l/a* = 5

S	Models	$\overline{w}$	$\overline{u}$	$\overline{v}$	$\overline{\sigma}_x\left(\alpha_3=\pm h/2\right)$	$\overline{\sigma}_\vartheta\left(\alpha_3=\pm h/2\right)$	$\overline{\sigma}_{x\vartheta}\left(\alpha_3=\pm h/2\right)$
100	**CST** (Soedel, 2004)	0.3291	-1.2223	-8.2812	1.7134	2.9345	0.1974
					-0.1656	-2.8966	-0.4390
	FSDT (Khdeir et al., 1989)	0.3381	-1.2552	-8.5078	1.7596	3.0134	0.2017
					-0.1705	-2.9751	-0.4521
	Present Study (1)	0.3753	-1.3934	-9.4436	1.8901	3.1335	0.2129
					-0.1274	-3.0977	-0.4899
	(2)	0.3381	-1.2552	-8.5078	1.7599	3.0134	0.2018
					-0.1702	-2.9751	-0.4519
	HSDT (Nwoji et al., 2021)	0.3288	-1.2205	-8.2721	1.7099	2.9273	0.1961
					-0.1647	-2.8892	-0.4388
20	**CST** (Soedel, 2004)	0.4025	-0.2990	-2.0255	1.3384	3.5703	0.3596
					-0.9599	-3.5610	-0.4187
	FSDT (Khdeir et al., 1989)	0.4069	-0.3021	-2.0478	1.3420	3.5750	0.3596
					-0.9593	-3.5652	-0.4200
	Present Study (1)	0.4615	-0.3446	-2.3297	1.4372	3.7675	0.3953
					-1.0203	-3.8221	-0.4609
	(2)	0.4069	-0.3021	-2.0478	1.3420	3.5750	0.3597
					-0.9592	-3.5652	-0.4198
	HSDT (Nwoji et al., 2021)	0.4071	-0.3023	-2.0488	1.3413	3.5728	0.3594
					-0.9586	-3.5634	-0.4195
10	**CST** (Soedel, 2004)	0.4053	-0.1505	-1.0199	1.2525	3.5930	0.3770
					-1.0619	-3.5883	-0.4068
	FSDT (Khdeir et al., 1989)	0.4212	-0.1564	-1.0600	1.2565	3.5939	0.3765
					-1.0586	-3.5892	-0.4077
	Present Study (1)	0.4784	-0.1817	-1.2187	1.3328	3.7582	0.4165
					-1.1419	-3.8833	-0.4465
	(2)	0.4212	-0.1564	-1.0599	1.2565	3.5939	0.3765
					-1.0585	-3.5892	-0.4077
	HSDT (Nwoji et al., 2021)	0.4242	-0.1575	-1.0674	1.2645	3.6167	0.3788
					-1.0652	-3.6119	-0.4101
4	**CST** (Soedel, 2004)	0.4061	-0.0603	-0.4088	1.1977	3.5986	0.3868
					-1.2131	-3.5968	-0.3986
	FSDT (Khdeir et al., 1989)	0.5052	-0.0748	-0.5084	1.2070	3.5988	0.3853
					-1.1120	-3.5964	-0.4002
	Present Study (1)	0.5758	-0.0958	-0.6172	1.2521	3.6652	0.4329
					-1.2289	-3.9893	-0.4366
	(2)	0.5052	-0.0750	-0.5085	1.2069	3.5985	0.3853
					-1.1120	-3.5965	-0.4003
	HSDT (Nwoji et al., 2021)	0.5245	-0.0779	-0.5279	1.2638	3.7696	0.4036
					-1.1651	-3.7669	-0.4191

Table 6 Non-dimensional deflection $\overline{w}$, in-plane displacements $\overline{u}$, $\overline{v}$; in-plane normal stresses $\overline{\sigma}_x$, $\overline{\sigma}_\vartheta$; in-plane shear stress $\overline{\sigma}_{x\vartheta}$ for simply supported (SS) circular cylindrical shell under sinusoidal loading (SDL) for *l/a* = 10

S	Models	$\overline{w}$	$\overline{u}$	$\overline{v}$	$\overline{\sigma}_x\left(\alpha_3=\pm h/2\right)$	$\overline{\sigma}_\vartheta\left(\alpha_3=\pm h/2\right)$	$\overline{\sigma}_{x\vartheta}\left(\alpha_3=\pm h/2\right)$
100	**CST** (Soedel, 2004)	0.4146	-0.8028	-10.3856	1.3692	3.6549	0.1806
					-0.8638	-3.6517	-0.2204
	FSDT (Khdeir et al., 1989)	0.4185	-0.8100	-10.4820	1.3815	3.6876	0.1821
					-0.8713	-3.6841	-0.2226
	Present Study (1)	0.4755	-0.9206	-11.9094	1.4889	3.9202	0.1999
					-0.9133	-3.9308	-0.2453
	(2)	0.4185	-0.8102	-10.4822	1.3816	3.6876	0.1822
					-0.8712	-3.6841	-0.2224
	HSDT (Nwoji et al., 2021)	0.4152	-0.8037	-10.3974	1.3691	3.6539	0.1805
					-0.8632	-3.6508	-0.2204
20	**CST** (Soedel, 2004)	0.4211	-0.1630	-2.1092	1.1850	3.7100	0.1995
					-1.0824	-3.7093	-0.2076
	FSDT (Khdeir et al., 1989)	0.4253	-0.1647	-2.1303	1.1859	3.7114	0.1996
					-1.0822	-3.7104	-0.2078
	Present Study (1)	0.4837	-0.1883	-2.4302	1.2598	3.9230	0.2205
					-1.1611	-3.9887	-0.2283
	(2)	0.4253	-0.1647	-2.1302	1.1860	3.7114	0.1996
					-1.0822	-3.7104	-0.2078
	HSDT (Nwoji et al., 2021)	0.4259	-0.1649	-2.1334	1.1866	3.7132	0.1997
					-1.0828	-3.7126	-0.2079
10	**CST** (Soedel, 2004)	0.4213	-0.0816	-1.0551	1.1599	3.7116	0.2017
					-1.1086	-3.7113	-0.2057
	FSDT (Khdeir et al., 1989)	0.4376	-0.0848	-1.0955	1.1610	3.7119	0.2016
					-1.1077	-3.7117	-0.2059
	Present Study (1)	0.4978	-0.0985	-1.2620	1.2219	3.8906	0.2238
					-1.1997	-4.0231	-0.2256
	(2)	0.4375	-0.0847	-1.0956	1.1610	3.7118	0.2016
					-1.1077	-3.7117	-0.2058
	HSDT (Nwoji et al., 2021)	0.4406	-0.0853	-1.1035	1.1686	3.7361	0.2029
					-1.1149	-3.7357	-0.2071
4	**CST** (Soedel, 2004)	0.4213	-0.0326	-0.4221	1.1447	3.7120	0.2029
					-1.1241	-3.7119	-0.2045
	FSDT (Khdeir et al., 1989)	0.5223	-0.0404	-0.5232	1.1471	3.7121	0.2027
					-1.1217	-3.7119	-0.2048
	Present Study (1)	0.5964	-0.0516	0.6353	1.1775	3.7910	0.2286
					-1.2446	-4.1227	-0.2234
	(2)	0.5223	-0.0404	-0.5232	1.1471	3.7119	0.2028
					-1.1217	-3.7118	-0.2048
	HSDT (Nwoji et al., 2021)	0.5420	-0.0420	-0.5430	1.2005	3.8852	0.2122
					-1.1741	-3.8851	-0.2143

Table 7 presents the through thickness distribution of the non-dimensional transverse shear stresses obtained by the FSODM and SSODM theories. Though the strain field (Eq. (2.11)) of the FSODM theory; together with the obtained results depicts that of a parabolic distribution of the transverse shear, this nevertheless results in only a slight improvement over the constant transverse shear distribution of the first-order shear deformation theory (FSDT) and linear transverse shear distribution of the present SSODM theory. The present FSODM and SSODM theories ultimately

succumb to same drawback as the FSDTs due to their inability to satisfy the zero transverse shear/traction surface condition.

Table 7 Thickness distribution of the non-dimensional transverse shear stresses $\overline{\sigma}_{xz}$ and $\overline{\sigma}_{\vartheta z}$ for the moderately thick (S =10) simply supported circular cylindrical shell under SDL

				Thickness coordinate $\alpha_3 = zh$						
	z			**-1/2**	**-1/3**	**-1/6**	**0**	**1/6**	**1/3**	**1/2**
***l/a*=0.5**	**HSDT** (Nwoji et al., 2021)		$\overline{\sigma}_{xz}$	0	0.78150	1.24630	1.40127	1.24630	0.78150	0
			$\overline{\sigma}_{\vartheta z}$	0	-0.49710	-0.79274	-0.89133	-0.79274	-0.49710	0
	Present study	**(1)**	$\overline{\sigma}_{xz}$	0.95230	0.95190	0.95170	0.95159	0.95163	0.95181	0.95214
			$\overline{\sigma}_{\vartheta z}$	-0.59828	-0.59803	-0.59787	-0.59780	-0.59782	-0.59794	-0.59814
		(2)	$\overline{\sigma}_{xz}$	0.94196	0.94193	0.94190	0.94187	0.94183	0.94180	0.94177
			$\overline{\sigma}_{\vartheta z}$	-0.60010	-0.60008	-0.60006	-0.60004	-0.60002	-0.60000	-0.59997
	FSDT (Khdeir et al., 1989)		$\overline{\sigma}_{xz}$	0.94100	0.94100	0.94100	0.94100	0.94100	0.94100	0.94100
			$\overline{\sigma}_{\vartheta z}$	-0.60000	-0.60000	-0.60000	-0.60000	-0.60000	-0.60000	-0.60000
***l/a*=5**	**HSDT** (Nwoji et al., 2021)		$\overline{\sigma}_{xz}$	0	0.32058	0.51124	0.57481	0.51124	0.32058	0
			$\overline{\sigma}_{\vartheta z}$	0	-2.03007	-3.23743	-3.64000	-3.23743	-2.03007	0
	Present study	**(1)**	$\overline{\sigma}_{xz}$	0.41244	0.41224	0.41210	0.41202	0.41200	0.41205	0.41216
			$\overline{\sigma}_{\vartheta z}$	-2.59168	-2.59069	-2.59010	-2.59991	-2.59010	-2.59068	-2.59167
		(2)	$\overline{\sigma}_{xz}$	0.38005	0.38001	0.37997	0.37993	0.37989	0.37984	0.37980
			$\overline{\sigma}_{\vartheta z}$	-2.43370	-2.43369	-2.43369	-2.43368	-2.43367	-2.43367	-2.43366
	FSDT (Khdeir et al., 1989)		$\overline{\sigma}_{xz}$	0.37850	0.37850	0.37850	0.37850	0.37850	0.37850	0.37850
			$\overline{\sigma}_{\vartheta z}$	-2.43380	-2.43380	-2.43380	-2.43380	-2.43380	-2.43380	-2.43380
***l/a*=10**	**HSDT** (Nwoji et al., 2021)		$\overline{\sigma}_{xz}$	0	0.16276	0.25956	0.29183	0.25956	0.16276	0
			$\overline{\sigma}_{\vartheta z}$	0	-2.07227	-3.30473	-3.71566	-3.30473	-2.07227	0
	Present study	**(1)**	$\overline{\sigma}_{xz}$	0.21174	0.21164	0.21156	0.21152	0.21151	0.21154	0.21159
			$\overline{\sigma}_{\vartheta z}$	-2.64958	-2.64858	-2.64798	-2.64777	-2.64797	-2.64858	-2.64958
		(2)	$\overline{\sigma}_{xz}$	0.19431	0.19429	0.19427	0.19425	0.19422	0.19420	0.19418
			$\overline{\sigma}_{\vartheta z}$	-2.48332	-2.48331	-2.48331	-2.48330	-2.48329	-2.48329	-2.48328
	FSDT (Khdeir et al., 1989)		$\overline{\sigma}_{xz}$	0.19310	0.19310	0.19310	0.19310	0.19310	0.19310	0.19310
			$\overline{\sigma}_{\vartheta z}$	-2.48340	-2.48340	-2.48340	-2.48340	-2.48340	-2.48340	-2.48340

The SSODM theory has been found to provide a better behavioral response to the static bending deformation of the thin and moderately thick shell, with recorded results in close agreement with those of the CST (thin shell cases only); FSDT; HSDT. The FSODM theory predicts generally higher values of displacements and stresses for both thin and thick shells alike, with very few instances of notable exception when compared to those of the CST; FSDT; HSDT at high ratios of length to radius of curvature (l/a = 2.5 – 10). The addition of the terms $u\frac{\alpha_3}{R_1}$ and $v\frac{\alpha_3}{R_2}$ in the Taylor (polynomial) series expansions of the mid-surface displacement components as quadratic functions of the thickness coordinate as in the SSODM; together with the adoption of the modified form of the transverse shear strain–displacement relations (Eq. (2.64)) by Reddy and Liu (1985) has been found to ensure the validity of the Love–Kirchhoff kinematic hypothesis of negligible transverse shear effect on the bending deformation of thin isotopic shells when in use of the second-order shear deformation theory of polynomial displacement models.

5 CONCLUSIONS

In this study, two second-order shear deformation theories (SSDTs) were developed from two variant forms of the polynomial second-order displacement models to predict the static bending response of thin and moderately thick isotropic shells. This was achieved by introducing the second-order displacement models into the kinematic relations of linear elasticity; together with the use of the material constitutive relations. The theory formulated on the first second-order displacement model (FSODM) accounts for a quadratic distribution of the transverse shear through the shell thickness. While the theory formulated on the second second-order displacement model (SSODM) accounts for a linear through thickness distribution of the transverse shear, though the condition of a traction free surface on the top and bottom of the shell was violated by both theories. The developed SSDTs were then applied to the particular case of circular cylindrical shells; the analytical solutions were obtained for simply supported boundary conditions using the Navier solution technique. Numerical results were generated and comparisons were made to those of the classical shell theory (CST), first-order shear deformation theory (FSDT) and higher-order shear deformation theory (HSDT) to ascertain the efficacy of the adopted displacement models. It was observed that the results of the SSDTs formulated on the FSODM and SSODM were in close agreement with those of the CST; FSDT; HSDT for the thin circular cylindrical shell and equally close with the FSDT; HSDT for the moderately thick shell at low ratio of length to radius of curvature. The accuracy of the theory formulated on the FSODM in predicting acceptable values of displacements and stresses in thin shells was found to significantly diminish with continual increase in length to radius of curvature ratios. However, this limitation was not shared by the theory formulated on the SSODM. The present SSODM theory was found to predict the results of the static bending deformation of the thin and moderately thick shell in close agreement with those of the FSDT; HSDT regardless of the length to radius of curvature ratios considered.

Author's Contributions: Conceptualization, CU Nwoji and DG Ani; Methodology, CU Nwoji and DG Ani; Investigation, CU Nwoji and DG Ani; Writing - original draft, DG Ani; Writing - review & editing, CU Nwoji and DG Ani; Funding acquisition, CU Nwoji and DG Ani; Resources, CU Nwoji and DG Ani; Supervision, CU Nwoji.

Editor: Rogério José Marczak

References

Ali, J. S., Alsubari, S., Aminanda, Y. (2015). A higher order theory for bending of cross ply laminated cylindrical shell under hygrothermal loads. Advanced Materials Research 1115: 509–512.

Amabili, M., Reddy, J. N. (2010). A new non-linear higher-order shear deformation theory for large-amplitude vibrations of laminated doubly curved shells. Int. J. Non. Linear. Mech. 45: 4, 409–418.

Amabili, M., Reddy, J. N. (2020). The nonlinear, third-order thickness and shear deformation theory for statics and dynamics of laminated composite shells. Composite Structures 244: 112–265.

Cho, M., Kim, K. O., Kim, M. H. (1996). Efficient higher-order shell theory for laminated composites. Composite Structures 34: 2, 197–212.

Di, S. and Rothert, H. (1995). A solution of laminated cylindrical shells using an unconstrained third-order theory. Computers and Structures 69: 3, 291–303.

Ghugal, Y. M., Shimpi, R. P. (2002). A Review of Refined Shear Deformation Theories of Isotropic and Anisotropic Laminated Plates. Journal of Reinforced Plastics and Composites 21: 9, 775–813.

Harle, S. M., Asha, A. V. (2013). Vibration and buckling of circular cylindrical panels by higher order shear deformation theory. International Journal of Engineering Research & Technology 2: 145–164.

Khdeir, A. A., Reddy, J. N., Frederick, D. (1989). A study of bending, vibration and buckling of cross-ply circular cylindrical shells with various shell theories. Int. J. Eng. Sci. 27: 11, 1337–1351.

Khdeir, A. A., Reddy, J. N. (1999). Free vibration of laminated composite plates using second-order shear deformation theory. Computer and Structures 71: 617–626.

Leissa, A. W. (1973). Vibration of Shells. NASA SP-288 National Aeronautics and Space Administration (Washington D. C.).

Lim, C. W., Liew, K. M. (1995). A higher order theory for vibration of shear deformable cylindrical shallow shells. Int. J. Mech. Sci. 37: 3, 277–295.

Mindlin, R. D. (1951). Influence of rotary inertia and shear on flexural motion of isotropic, elastic plates. Journal of Applied Mechanics 18: 31–38.

Naghdi, P. M. (1957). On the Theory of Thin Elastic Shells. Quaterly of Applied Mathematics 14: 339–380.

Nelson, R. B., Lorch, D. R. (1974). A Refined Theory for Laminated Orthotropic Plates. ASME Journal of Applied Mechanics 41: 177–183.

Nosier, A., Reddy, J. N. (1992). Vibration and stability analyses of cross-ply laminated circular cylindrical shells. Journal of Sound and Vibration 157: 1, 139–159.

Nwoji, C. U., Ani, D.G., Oguaghamba, O. A., Ibeabuchi, V. T. (2021). Static bending of isotropic circular cylindrical shells based on the higher order shear deformation theory of Reddy and Liu. Int. J. of Applied Mechanics and Engineering 26: 3, 141–162.

Oktem, A. S., Chaudhuri, R. A. (2007). Levy type fourier analysis of thick cross–ply doubly curved panels. Composite Structures 80: 475–488.

Onyeka F. C., Okafor, F. O., Onah, H. N. (2018). Displacement and Stress Analysis in Shear Deformable Thick Plate. International Journal of Applied Engineering Research 13: 11, 9893-9908.

Pister, K. S., Westmann, R. A. (1962). Bending of Plates on an Elastic Foundation. ASME Journal of Applied Mechanics 29: 2, 369–374.

Reddy, J. N. (1984). A simple higher-order theory for laminated composite plates. ASME Journal of Apllied Mechanics 51: 745–752.

Reddy, J. N. (2007). Theory and Analysis of Elastic Plates and Shells. Taylor & Francis group (London).

Reddy, J. N., Arciniega, R. A. (2004). Shear deformation plate and shell theories: from Stavsky to present. Mechanics of Advanced Materials and Structures 11: 535–582.

Reddy, J. N., Liu, C. F. (1985). A higher-order shear deformation theory of laminated elastic shells. International Journal of Engineering Science 23: 3, 319–330.

Shahrjerdi, A., Bayat, M., Mustapha, F., Sapuan, S. M., Zahari, R. (2010). Second-Order Shear Deformation Theory to Analyze Stress Distribution for Solar Functionally Graded Plates. Mechanics Based Design of Structures and Machines: An International Journal 38: 3, 348–361.

Shahrjerdi, A., Mustapha, F. (2011). Second Order Shear Deformation Theory (SSDT) for Free Vibration Analysis on a Functionally Graded Quadrangle Plate. In Dr. Natalie Baddour (Ed.), Recent Advances in Vibrations Analysis (59–78). In Tech.

Shahrjerdi, A., Mustapha, F., Bayat, M., Majid, D. L. A. (2011). Free vibration analysis of solar functionally graded plates with temperature-dependent material properties using second order shear deformation theory. Journal of Mechanical Science and Technology 25: 9, 2195–2209.

Soedel, W. (2004). Vibrations of Shells and Plates. Marcel Dekker, Inc (New York).

Soldatos, K. P. (1986). On thickness shear deformation theories for the dynamic analysis of non-circular cylindrical shells. International Journal of Solids Structures 22: 6, 625–641.

Szekrenyes, A. (2013). Interface fracture in orthotropic composite plates using second-order shear deformation theory. International Journal of Damage Mechanics 22: 8, 1161–1185.

Timoshenko, S., Woinowsky – Krieger, S. (1987). Theory of Plates and Shells. McGraw – Hill (New York).

Ugural, A. C. (2010). Stresses in Beams, Plates, and Shells, Third Edition. CRC Press - Taylor & Francis Group (New York).

Viola, E., Tornabene, F., Fantuzzi, N. (2013). General higher-order shear deformation theories for the free vibration analysis of completely doubly-curved laminated shells and panels. Composite Structures 95: 639–666.

Whitney, J. M., Sun, C. T. (1973). A Higher Order Theory for Extensional Motion of Laminated Composites. Journal of Sound and Vibration 30: 1, 85–97.